Functional diversification of the four MARCKS family members in zebrafish neural development

Journal:	*JEZ Part B: Molecular and Developmental Evolution*
Manuscript ID	JEZ-B-2016-01-0083.R1
Wiley - Manuscript type:	Research Article
Date Submitted by the Author:	n/a
Complete List of Authors:	Prieto, Daniel; Institut Pasteur de Montevideo, Recombinant Proteins Unit; Universidad de la Republica Uruguay Facultad de Ciencias, Sección Biología Celular Zolessi, Flavio; Universidad de la Republica Uruguay Facultad de Ciencias, Sección Biología Celular; Institut Pasteur de Montevideo, Cell Biology of Neural Development lab
Keywords:	MARCKS, gene duplication, neurulation, retina, zebrafish, teleosts

Functional diversification of the four MARCKS family members in zebrafish neural development.

Daniel Prieto[1,3]; Flavio R. Zolessi[1,2,*]

[1] Sección Biología Celular, Facultad de Ciencias, Universidad de la República. Iguá 4225, Montevideo, 11400, Uruguay.

[2] Cell Biology of Neural Development Lab, Institut Pasteur de Montevideo. Mataojo 2020, Montevideo, 11400, Uruguay.

[3] Current address: Recombinant Proteins Unit, Institut Pasteur de Montevideo. Mataojo 2020, Montevideo, 11400, Uruguay.

Number of Figures: 7; Number of Supplementary Figures: 6

Number of Tables: 1; Number of Supplementary Tables: 6

Number of Supplementary Videos: 3

Abbreviated title: MARCKS proteins in zebrafish development

***Corresponding Author:** Flavio R. Zolessi

Cell Biology of Neural Development Lab, Institut Pasteur de Montevideo.

Calle Mataojo 2020, Montevideo, 11400, Uruguay.

Tel.: +598 2522 0910; Fax: +598 2522 4185

Email: fzolessi@fcien.edu.uy / fzolessi@pasteur.edu.uy

Funding support: CSIC-UdelaR I+D grant C831-102; and PEDECIBA, Uruguay.

ABSTRACT

MARCKS and MARCKS-like 1, each encoded by a different gene, comprise a very small family of actin modulating proteins with essential roles in mammalian neural development. We show here that four genes (two *marcks* and two *marcksl1*) are present in teleosts including zebrafish, while ancient actinopterigians, sarcopterigian fishes and chondrichtyans only have two. No *marcks* genes were found in agnaths or invertebrates. All four zebrafish genes are expressed during development, and we show here how their early knockdown causes defects in neural development, with some phenotypical differences. Knockdown of *marcksa* generated embryos with smaller brain and eyes, while *marcksb* caused different morphogenetic defects, such as larger hindbrain ventricle and folded retina. *marcksl1a* and *marcksl1b* morpholinos also caused smaller eyes and brain, although *marcksl1a* alone generated larger brain ventricles. At 24 hpf, *marcksb* caused a wider angle of the hindbrain walls, while *marcksl1a* showed a "T-shaped" neural tube and alterations in neuroepithelium organization. The double knockdown surprisingly produced new features, that included an increased neuroepithelial disorganization and partial neural tube duplications evident at 48 hpf, suggesting defects in convergent extension. This disorganization was also evident in the retina, although retinal ganglion cells were still able to differentiate. *marcksl1b* morphants presented a unique retinal phenotype characterized by the occurrence of sporadic ectopic neuronal differentiation. Although only *marcksl1a* morphant had a clear "ciliary phenotype", all presented significantly shorter cilia. Altogether, our data show that all *marcks* genes have functions in zebrafish neural development, with some differences that suggest the onset of protein diversification.

KEYWORDS

MARCKS, gene duplication, neurulation, retina, zebrafish, teleosts

INTRODUCTION

Gene duplication is a major mechanism for the generation of novel genes in evolution (Reams and Roth, 2015). During the evolution of vertebrates, two consecutive genome duplications are thought to have occurred before the separation of teleost fishes from tetrapods, followed by a third whole genome duplication, usually known as 3R or FSGD (fish-specific genome duplication), just in the lineage of actinopterigians around 350 mya (Glasauer and Neuhauss, 2014). Despite a common characteristic of most gene duplication events being that one of the two duplicates eventually degenerates as a pseudogene and functionally disappears, it has been found that in zebrafish most duplicated genes have been maintained (Taylor et al., 2003), greatly increasing the genomic complexity of this species. It has been a matter of debate whether this further genome duplication might be responsible for the great evolutionary success of ray-finned fishes with their broad species diversity (Glasauer and Neuhauss, 2014). However, it is clear that the maintenance of several copies of a gene greatly increases the probability that new functions arise in the encoded proteins, and that the magnitude of this probability would depend on the peculiarities of the individual set of proteins. MARCKS is a family of proteins with only two members in tetrapods, MARCKS (Myristoylated Alanin-Rich C-Kinase Substrate) and MARCKS-like 1 (MARCKSL1, also known as MARCKS-Related Protein/MRP or MARCKS-Like Protein/MLP). Both are ubiquitously expressed although massively enriched in neural tissues (Ouimet et al., 1990), and have been reported to be essential for a plethora of processes related to neural development as has been nicely shown by loss-of-function experiments (Stumpo et al., 1995; Chen et al., 1996). Their genes have been studied, and their mechanisms of regulation at the transcriptional level have been characterized to some extent; humans, as well as mice have very large mature *marcks* transcripts encoding small proteins, thus having a high percentage of non-coding sequences, with a remarkable >1kb segment at the 3'-untranslated region generally assumed to be related to gene expression regulatory sites (see for example Stumpo et al., 1998). The protein sequence, with around 250-300 residues, presents only

three relatively well-conserved domains (Li and Aderem, 1992; Blackshear, 1993): a short N-terminal myristoylation-site domain; a 20-25-residues 'MARCKS homology 2' domain (MH2), coincident with the mRNA region surrounding the only splicing site; and another 25-residues 'effector domain' (ED), with three serines phosphorylatable by PKC and able to interact with the plasma membrane, F-Actin and calcium-Calmodulin. Of these, the MH2 domain appears as the most puzzling, as no function could yet be ascribed to it. Our group has demonstrated that it contains an extremely conserved serine residue, S25, which in the chick embryo is phosphorylated by Cdk5 in neuroblasts, some neurons and some migrating neural crest cells, and that this phosphorylation depends on the integrity of the actin cytoskeleton and on cell-to-cell adhesion (Zolessi and Arruti, 2001a; Zolessi et al., 2004; Toledo and Arruti, 2009; Ruiz-Perera et al., 2013; Toledo et al., 2013).

However, probably one of the most remarkable peculiarities of these proteins is that they are, along nearly all their polypeptide extension, naturally unfolded (see for example Tapp et al., 2005). Their protein sequences are rather unique reflecting this feature: not only they show a relatively uncommon mixture of charged residues, being extremely hydrophilic and with a pI of around 4.0, but they are also enriched in some aminoacids such as alanine, glutamic acid and proline, and lack some other ones such as tyrosine, tryptophan, cysteine and methionine (the initial one being post-translationally removed in cells) (Li and Aderem, 1992; Blackshear, 1993). As it is usually seen in naturally unfolded polypeptides, MARCKS proteins sequence is poorly conserved across species (Tinoco et al., 2014).

In addition to the two previously described MARCKS encoding genes (Ott et al., 2011), we have found two MARCKSL1-encoding genes in the zebrafish and performed a comparative characterization of their genomic, mRNA and predicted protein primary structures, in addition to functionally testing them by using specific morpholino antisense oligomers. Our phenotypic analyses of morphant embryos show that even if they have similarities, like the previously described smaller head and eyes and curved body, there are essential differences in neurulation,

brain and eye morphogenesis and neuronal differentiation. Interestingly, some *marcks* genes seem to interact in different developmental processes. These observations suggest that MARCKS proteins sequence peculiarities have allowed them to distribute their functions in neural development among the four members of the family, representing what could be the onset of protein diversification and eventual acquisition of novel functions.

MATERIALS AND METHODS

Sequence analysis

MARCKS and MARCKSL1 protein and genomic sequences from several different vertebrates, including zebrafish, were obtained either through name search or by BLAST/BLAT (Altschul et al., 1990; Kent, 2002) using as a bait whole or partial protein sequences from previously well-characterized *marcks* genes (such as human or chick) against different databases in NCBI (http://www.ncbi.nlm.nih.gov) or Ensembl (http://www.ensembl.org). Genomic sequences were obtained by BLAST/BLAT alignment against genomic assembly. For generating figures, sequences were aligned with a global algorithm using ClustalW2 (Larkin et al., 2007) or Clustal Omega (Sievers et al., 2011) and further processed using BioEdit (http://www.mbio.ncsu.edu/bioedit/bioedit.html). Phylogeny reconstruction was made using the tools available at Phylogeny.fr (http://www.phylogeny.fr/; Dereeper et al., 2008), such as MUSCLE (Edgar, 2004) for multiple sequence alignment, PhyML (Guindon et al., 2010) for maximum-likelihood phylogeny and TreeDyn (Chevenet et al., 2006) for tree visualization and export. Trees were further processed using MEGA 6 (Tamura et al., 2013), bootstrapping with 1000 iterations using Tamura-Nei algorithm (Tamura and Nei, 1993); branches with statistical support lower than 0.5 were collapsed. Relative time tree analyses were conducted in MEGA7 (Kumar et al., 2016), using the Tamura-Nei model and the RelTime method to infer time trees when needed (Tamura et

al., 2012). CpG islands prediction was performed within the -1kb genomic region with the software EMBOSS Cpgplot (Larsen et al., 1992; McWilliam et al., 2013) within a 200 bp window, reporting putative islands when larger than 50 bp. Myristoylation probability was analyzed using NMT – The MYR Predictor (Maurer-Stroh et al., 2002). GC content analysis was performed in R/Bioconductor using the package seqinr (Gentleman et al., 2004; Lawrence et al., 2013).

RT-PCR and qRT-PCR

RNA was extracted from a pool of whole embryos at different stages with TriZol, and first strand cDNA was synthesized from 200 ng total RNA with MMLV-RT (Fermentas-Thermo Scientific, Waltham, USA) using an oligo dT_{18-20} primer. Hot start PCR reactions were carried out with primers detailed in Table S1. Real-time qRT-PCR reactions were performed using Kapa SYBR Fast qPCR kit (Kapa Biosystems, Wilmington, USA) following the protocol suggested by the manufacturer, using a Corbett 6000 (Qiagen, Venlo, Netherlands) thermal cycler. Two reference genes were used: *rpl13a* and *ef1a*, as suggested for developmental processes (Tang et al., 2007). Data processing of triplicate experiments were analyzed with the software REST 2009 (Qiagen, Venlo, Netherlands), normalizing primer pair efficiency (Pfaffl, 2004). Oocyte cDNA was established as the control group. Primers used are detailed in Table S1.

Zebrafish embryos and morpholino oligomere treatments

Zebrafish lines were kept under controlled conditions, in an automated ZebTec (Tecniplast, Milan, Italy) stand-alone system at 28 °C, 500 µS/cm^2 conductivity and a pH of 7.5, and fed with dry and live food (*Artemia salina*) three times a day, following accepted protocols and under the approval of the local and national ethical committees (CEUA at Institut Pasteur de Montevideo, CHEA-UdelaR and CNEA). SAT wild-type line used for most experiments was obtained from ZIRC (Eugene,

USA). The transgenic line Atoh7:Gap43-EGFP (Atoh7:GFP in the text), in which cells leading to the retinal ganglion cells lineage are labeled (Zolessi et al., 2006), was obtained from Bill Harris' lab, University of Cambridge, UK. Embryos obtained from natural crossings were cultured at 28.5 °C in E3 medium (5 mM NaCl; 0.17 mM KCl; 0.33 mM $CaCl_2$; 0.33 mM $MgSO_4$) supplemented with 0.1 mM phosphate buffer and methylene blue (1 ppm) as a fungostatic. 1-phenyl-2-thiourea (0.003%) was added to E3 medium to inhibit melanogenesis in embryos destined to microscopy imaging.

Translation-blocking morpholino antisense oligomers (MOs; Gene Tools, Philomath, USA, or Open Biosystems - now GE Healthcare Dharmacon, Lafayette, USA) were designed against 5' untranslated region (5'-UTR) of *marcksa*, *marcksb*, *marcksl1a* and *marcksl1b*, and a splice-blocking MO was designed against the donor sequence of the only *marcksl1a* intron (for sequences see Table S1). Standard control MOs (Gene Tools, Philomath, USA) were used as appropriate. To prevent unspecific cell death that could hinder the specific phenotypes, and particularly in double MO injections, we co-injected a double amount per embryo of the standard anti-p53 MO (Robu et al., 2007). MOs were injected in the yolk at 1 to 8 cells stage, and embryos were cultured as described above until the desired stage. Specific function-recovery controls were performed by co-injecting the corresponding synthetic mRNAs lacking the morpholino recognition site, produced from PCR templates with Ambion mMESSAGE mMACHINE (Thermo-Fisher, Waltham, USA). Primers used are described in Table S1.

Histology and morphological observations

Alcian Blue staining: 5 dpf embryos were fixed with 4% PFA for 24h, washed 5 times in PTw (PBS/ 0.1% Tween-20) and stained overnight with Alcian blue (0.1% Alcian blue in 70% ethanol/ 1% hydrochloric acid). Embryos were rinsed 4 times in acid alcohol (70% ethanol/ 5% hydrochloric

acid) and then incubated for 20 min in acid alcohol at room temperature. Rehydration was performed in gradually decreasing solutions of acid alcohol/water (3:1, 1:1, 1:3) and finally rinsed in water. Embryos were then clarified and stored in 50% glycerol/ 0.5% KOH as previously described (Solomon et al., 2003).

Semithin sectioning and methylene blue staining: 48 hpf zebrafish embryos were fixed in 2.5% glutaraldehyde. After 10 min, heads were dissected and then fixed for 48 h at 4° C. Fixative was removed and embryos postfixed with OsO_4, and then dehydrated and embedded in araldite (Durcupan; Fluka-Sigma-Aldrich, St. Louis, USA). Semithin sections (0.5 µm thick) were obtained in an ultramicrotome RMC MT-X (Boeckeler Instruments, Tucson, USA), dried over the flame and stained with 1% methylene blue.

Immunostaining and fluorescence microscopy

Dechorionated 24, 48, 72 hpf and 5 dpf embryos treated with PTU were fixed with 4% PFA, permeabilized with 5 washes of 30 min each with PBS-T (PBS/0.2% Triton X-100) and trypsinized on ice for 15 - 30 min. After washing with PBS-T on ice, embryos were incubated in blocking solution (10% normal goat serum, 1% BSA, 10% glycine, 0.2% NaN3 in PBS-T). Primary antibody was incubated in blocking solution overnight at 4 °C, with gentle agitation. Then, five washes with PBS-T for 30 min at 4 °C with gentle agitation were performed, and the corresponding secondary antibody was incubated overnight with gentle agitation, adding when necessary 2 µg/mL methyl green as a DNA-specific nuclear stain (Prieto et al., 2014) or 1 µg/mL TRITC-phalloidin (Sigma, St. Louis, USA) to label F-Actin. After washing, embryos were mounted in glycerol solution (75% glycerol/20 mM Tris pH=8). Zn-5 antibody against Neurolin-a/DM-GRASP (a retinal ganglion cell -RGC- marker; Trevarrow et al., 1990; Schmitt and Dowling, 1994) and Zpr-1 antibody against Arrestin 3a, a double cone (DC) marker (both mouse monoclonals from ZIRC, Eugene, USA) were

used as hybridoma supernatant at 1:100 dilution. Anti-aPKC rabbit polyclonal antibody was obtained from Santa Cruz (Dallas, USA), and used in a 1:200 dilution. Anti-Gamma Tubulin and anti-acetylated Tubulin monoclonal antibodies (IgG1 and IgG2b, respectively) were from Sigma (St. Louis, USA) and, when necessary, detected simultaneously using isotype-specific Alexa fluorescently-labelled secondary antibodies from Molecular Probes-Life Technologies (Carlsbad, USA). Image acquisition was made in a Leica TCS-SP5 laser scanning confocal microscope using LASAF v. 2 software (Leica Microsystems, Wetzlar, Germany). Further image analysis, including quantification, and processing for figures and videos were made using Fiji (http://fiji.sc/) (Schindelin et al., 2012).

RESULTS

Four *marcks* family genes in zebrafish

Two *marcks* genes (*marcksa* and *marcksb*) have been previously identified in the zebrafish by sequence comparison to the human *marcks* cDNA sequence (Ott et al., 2011). The analysis of the respective genome sequences showed us that while *marcksb* gene contains only one intron at the position described for other species (Blackshear, 1993), *marcksa* gene has two introns: the first one localized at the usual position coincident with the MH2 domain, and the second one at the 3' UTR (Fig. 1A and Table 1). Furthermore, there is a 12-nucleotide shift in the 5' donor site of the first splicing site of *marcksa*, resulting in the addition of four residues to the protein sequence in a region (the MH2 domain) that is highly conserved in all vertebrates (Fig. S1 and S2). In an attempt to characterize the whole *marcks* family in the zebrafish, we further searched for other sequences by performing a BLAST ("tblastn") search on the NCBI Nucleotide collection (nr/nt) using as a bait the amino-terminal half including the ED (residues 1-135) of zebrafish MARCKSA protein

sequence (accession code AAH95101.1). In addition to the already described *marcksb* gene, we found two putative *marcksl1* sequences, namely *marcksl1a* and *marcksl1b* (GenBank transcript accession numbers NM_213223 and NM_213133 respectively). These sequences have more recently been annotated in an exactly opposite way, although several features of the predicted protein sequences makes us propose that the gene currently annotated as *marcksl1b* (NM_213223) is the one which should be named *marcksl1a*, and viceversa. The main reason for this proposal is overall sequence homology: the *marcksl1a* transcript (NM_213223) is around 44-48% identical to that of other vertebrates, while *marcksl1b* transcript (NM_213133) identity is around 38-40% (Table S2). In addition, in the one we call *marcksl1a*, some key protein regions are more conserved when compared to other *marcksl1* proteins, such as the myristoylatable amino-terminus sequence "GSQ" (against "GAQ" for *marcksl1b*) (Fig. S1 and S2). *marcksl1a* maps to chromosome 19 and *marcksl1b* to chromosome 13, and their genes are interrupted by only one intron of 1150 and 1340 bp respectively (Fig. 1A and Table 1). The same analysis performed with *marcksa* and *marcksb* sequences showed us that while *marcksb* gene contains only one intron at the position described for other species (Blackshear, 1993), *marcksa* gene has two introns: the first one localized at the usual position coincident with the MH2 domain, and the second one at the 3' UTR (Fig. 1A and Table 1). Furthermore, there is a 12-nucleotide shift in the 5' donor site of the first splicing site of *marcksa*, resulting in the addition of four residues to the protein sequence (Fig. S1 and S2). At the protein level, the zebrafish *marcksl1* sequences encode typical MARCKS family proteins abundant in alanine, lysine and glutamic acid residues, while lacking arginine, methionine, cysteine, tryptophan or tyrosine residues. Both present a myristoylatable glycine residue in a consensus sequence at the amino terminus. They also present identifiable MH2 and effector (ED) domains, and several potentially phosphorylatable serine and threonine residues which scored a high probability of phosphorylation when analyzed within their context (Fig. S1 and Table S3).

Aiming at establishing the evolutionary relationships of the *marcks* family genes identified in the zebrafish, we collected the predicted protein sequences available in public protein and genomic

databases, such as NCBI and Ensembl, for several other species of vertebrates, using either keyword ("marcks") or homology searches (using MARCKS proteins conserved regions as a bait against translated genomic or transcript databases). In addition to some previously published sequences such as those from human (Harlan et al., 1991; Stumpo et al., 1998), mouse (Seykora et al., 1991; Umekage and Kato, 1991), and chick (Graff et al., 1989), we found genes encoding MARCKS family proteins from several other species, ranging from cartilaginous fishes to mammals (Table S4). Even if there are relatively complete genome or transcriptome sequences for several invertebrates, protochordates and even agnaths, we failed to find any homologs in these species. We found that there are only two *marcks* family genes (*marcks* and *marcksl1*) not only in tetrapods, but also in the sarcopterigian fish coelacanth (*Latimeria chalumnae*), in the cartilaginous fish elephant shark (*Callorhinchus milii*) and in the ancient actinopterigian spotted gar (*Lepisosteus oculatus*). Conversely, all teleosts for which we could find complete or reliable sequences (either from genome or cDNA) have at least four *marcks* family genes, like the zebrafish. Only *Tetraodon nigroviridis* appears to have five *marcks* genes in total, with a duplicated *marcksb* gene (Fig. 1B and Table S4). Using the predicted protein sequences for these genes, we have reconstructed a phylogenetic tree based on sequence alignment (Fig. 1B). Zebrafish MARCKS sequences grouped as expected with the corresponding predicted proteins in other species, with the apparent exception of the zebrafish MARCKSA, wich together with the medaka sequence, remained in the clade of all other MARCKS and MARCKSA sequences. To rule out whether their positioning in this complex phylogenetic tree was due to differences in zebrafish or medaka sequence change rates, or just an alignment artifact, we compared the genomic *marcks* or *marcksa* coding sequences from chondrychtian, actinopterigian and sarcopterigian fishes, using the human sequence as an outgroup (Table S5), and performed phylogeny reconstruction and time trees (Fig. S3). In both cases, these *marcksa* sequences grouped as expected, indicating similar substitution rates, which was further supported by maximum likelihood estimation of substitution rate at each site (not shown).

Comparison of *marcks* family genes expression in zebrafish

We have further explored the genomic sequences of all four *marcks* family genes aiming at identifying regulatory elements in the upstream regions up to 1kb. All four *marcks* family genomic and transcript sequences show a GC content higher than the zebrafish genome average of 36.5% (Table 1). Both *marcksa* and *marcksb* genomic sequences show CpG dimer enrichment in their 1 kb upstream sequences. While *marcksa* upstream region shows only one 124 bp GC-enriched region spanning positions -77 to -200 with 49% GC, *marcksb* upstream sequence shows two regions: one from position -58 to -135 with 54% GC content and the other one from position -276 to -355 with 59%. *marcksl1a* upstream region displays a similar enrichment from position -136 to -361 with 52% GC, whereas *marcksl1b* showed no detectable GC enrichment within the 1 kb upstream region (Fig. 2A). We observed that the presence of at least one GC-enriched region within the 1 kb upstream region is conserved among species for the *marcks* genes (Fig. 2A). Furthermore, the localization of this region between positions -50 to -200 also seems to be evolutionarily conserved. In teleost fishes there are one or two identifiable GC-enriched regions, and mammals display these regions in addition to at least one more region at the distal end (-650 to -800), which may have been secondarily acquired. A third distal GC enrichment was also found in the upstream sequence of the amphibian *Xenopus tropicalis*, although its position is more distal than those of mammals (Fig. 2A). Semi-quantitative RT-PCR showed us that all four genes were expressed in adult tissues (Fig. 2B). To better characterize the relative expression of each of these four genes along development, we performed real-time RT-PCR experiments, comparing them with two different house-keeping genes (*ef1a* and *rpl13a*) and using oocyte RNA levels as a reference. We confirmed that as described before (Ott et al., 2011) transcripts are present at all embryonic and larval stages. In the case of *marcksl* genes, they are also expressed at detectable levels between 24 and 72 hpf (Fig. 2C). Only

marcksa mRNA expression appeared to vary significantly within this interval, showing an apparently higher copy number by 24 hpf and a sustained decrease at 48 and 72 hpf. Meanwhile, neither *marcksb* nor *marcksl1a* or *marcksl1b* showed any evident variation within this developmental time period (Fig. 2C).

Morpholino knockdown of *marcks* family genes: effects on general embryo morphology

Two new translation-blocking MOs were designed against the zebrafish *marcks* mRNAs and injected in the yolk of embryos at stages 1-4 cells, at amounts between 0.3 and 0.6 pmol/embryo. *marcksa* MO injected embryos displayed gross anatomical defects similar to those previously described by Ott et al. for both genes using different MOs (Ott et al., 2011), like a shorter, curved body and smaller head and eyes (Fig. S4). However, the *marcksb* MO injected embryos showed some peculiarities not previously described, including severe optic cup malformation and enlargement of the hindbrain (fourth) ventricle, particularly noticeable at 48 hpf (Fig. S4A). These features were markedly reduced upon co-injection of a synthetic *marcksb* mRNA lacking the MO recognition site (Fig. S4C).

We also designed translation-blocking MOs to the two *marcksl1* genes and a splice-blocking MO to *marcksl1a*. As the translation MO to *marcksl1a* did not have any visible effect on development, probably due to genetic polymorphisms, we only show here results for the splice-blocking *marcksl1a* MO (Fig. S5). As this MO is directed to the donor site of the only intron in the *marcksl1a* transcript, it would only allow for the eventual expression of a truncated protein containing the first 28 residues, thus causing a null phenotype (Panizzi et al., 2007; Eisen and Smith, 2008). Similar to what was observed for *marcks* genes, knockdown of both *marcksl1* genes caused very visible defects in the central nervous system. Again, however, there are some evident differences between *marcksl1a* and *marcksl1b* morphants (Fig. 3A). Knockdown of *marcksl1a* at

relatively low doses of MO (0.2-0.4 pmol/embryo) provoked a strong phenotype characterized by smaller head and eyes, ventrally curved body and enlarged brain ventricles, that could be rescued by the concomitant injection of the *marcksl1a* synthetic mRNA (Fig. 3A and S5). *marcksl1b* MO, on the other hand, caused smaller head and eyes and curved body, but did not cause enlargement of ventricles (Fig. 3A).

As all four *marcks* morphants had apparent cephalic malformations, we wondered whether head cartilages were affected, and performed Alcian blue staining of embryos at 7 dpf (Fig. 3B). *marcksa* morphants showed impaired midline convergence of the ventrally-hanging Meckel cartilage, shortening of the palatoquadrate cartilages and rudimentary basihyal cartilages. *marcksb* morphants in turn showed anteriorly bent Meckel and palatoquadrate cartilages (Fig. 3B). Both depicted reduced ceratobranchial arches, a feature also observed in *marcksl1a* morphants. Major alterations in craniofacial cartilage development were not observed in *marcksl1b* morphants. The double *marcksl1a+marcksl1b* morphant elicited a phenotype with shortened palatoquadrate cartilages and reduced ceratobranchial arches resembling those of *marckls1a* morphants. All single morphants, as well as the double *marcksl1a+marcksl1b* morphant showed some extent of ceratohyal cartilage alteration (Fig. 3B-C).

Effect of *marcksb* and *marcksl1a* knockdown on the morphogenesis of the neural tube

As it has been shown that knockout of both *marcks* and *marcksl1* causes defects in cephalic neural tube closure in mice (Stumpo et al., 1995; Chen et al., 1996), and teleosts display a completely different mechanism for neurulation, we decided to compare the possible roles of the *marcks* family genes during zebrafish neurulation by morpholino knockdown. We performed single and double knockdown experiments, by injecting 0.4 pmol (total) of MO against the individual *marcks* family genes or a combination of *marcksb+marcksl1a* MOs (as these presented the strongest cephalic

morphology phenotypes), plus 0.8 pmol of *p53* MO per embryo. Embryos were then fixed, stained for F-actin and nuclei, and optically sectioned using a confocal microscope, to observe the transverse structure of the brain walls and ventricles at three areas: midbrain, anterior hindbrain (at the level of the first rhombomere) and posterior hindbrain (at the level of the inner ear) (Fig. 4A-E). We quantified these observations on hindbrain structure at 24 hpf by measuring the angle of the lateral walls around the floor plate, where a bending similar to the medial hinge-point of amniotes is evident in zebrafish embryos. Only when blocking the expression of *marcksb* alone there was a significantly larger angle (Fig. 4A-B). Conversely, a significantly smaller angle was observed for *marcksl1b* morphants (Fig. 4A), although this phenotype was also characterized by a pronounced delay in general development that might explain this observation. In *marcksl1a* morphants, even if there was not a significant change in the overall angle of the hindbrain walls, in many cases (9/17 embryos) there was a partial opening of the dorsal half, resulting in a "T-shaped" caudal neural plate (Fig. 4C and Video S1). In some regions along the hindbrain axis, the appearance of small groups of ectopic, supra-apical, cells was also evident in these embryos (Fig. 4C). At the level of the midbrain, only *marcksl1a* MO appeared to generate some deformation of the brain walls (Fig. 4C and Video S1).

These results indicating a major role for *marcksb* and *marcksl1a* in neural tube morphogenesis (when compared with the other two genes), prompted us to further compare their roles, by searching for possible complementation or interaction at the gene level. The simultaneous injection of both *marcksb* and *marcksl1a* morpholinos (at half dose each: 0.2 pmol/embryo), had a very strong effect on the general morphology of the embryos and on the brain, particularly evident on the midbrain section in Figure 4C. In these double *marcksb*+*marcksl1a* knockdown embryos, the overall morphology of the hindbrain regarding the angle of the lateral walls and the size/shape of the ventricle was similar to that of controls (Fig. 4A), indicating that they do not genetically interact to regulate ventromedial hingepoint angle in the hindbrain. However, new features appeared that were not evident in single morpholino injections. At early stages (24 hpf), the most evident one was a

visible disorganization of the neuroepithelium, marked by the ectopic accumulation of F-actin away from the apical surface (Fig. 4C and Video S1).

At 48 hpf the phenotype was maintained, albeit milder, in the *marcksb* morphants, while *marckls1a* morphants presented a more severe neuroepithelial disorganization, characterized by ectopic F-Actin accumulations (Fig. 4D and Video S2). The double morphant, on the other hand, showed an unexpected phenotype: the appearance of partial duplications of the neural tube from the hindbrain to the initial portion of the spinal cord (Fig. 4D and Video S2). A phenotype like this was never evident in *marcksb* morphants, but in a few extreme examples of *marcksl1a*-alone morphants at 24 hpf there was also evidence of a similar disorganization, although without a clear duplication of the neural tube (Fig. 4F and Video S3). In these *marcksl1a* morphant embryos, aPKC immunostaining revealed the ectopic localization of sub-apical protein complexes along with actin filaments that in some areas suggested early stages of partial neural tube duplication (Fig. 4F and Video S3) and indicated that the phenotype of the double morphants was most probably caused by *marcksl1a*, albeit facilitated by *marcksb* knockdown. More affected *marcksl1b* morphants also presented a similar phenotype, suggesting shared roles of the two zebrafish MARCKSL1 proteins during neural rod cavitation (Fig. 4F).

Morpholino knockdown of *marcks* family genes: effects on retinal development

marcks mutation in mice caused severe defects in retinal lamination (Stumpo et al., 1995), and a prominent general size reduction of the neural retina with a complete loss of the retinal layers was already reported for *marcks* knockdown in the zebrafish at 72 hpf (Ott et al., 2011). We hence decided to study the effect of *marcksl1* MOs in retinal morphology at different developmental stages. When looking at retinal structure, we found that both *marcksl1a* and *marcksl1b* MOs caused a severe delay in cell differentiation, as retinas had a very immature appearance even at 60 hpf,

when retinal layers were already evident in control embryos (Fig. 5). At 35 hpf RGCs (labeled by the monoclonal antibody zn-5), the first-born cell type in the retina, were just starting to differentiate in the control retinas, but were not detected in *marcksl1a* or *marcksl1b* morphants (Fig. 5A). At 60 hpf, when most retinal cell types are already born in normal development, the only cells that had evidently started differentiation in morphant embryos were RGCs, and they were much fewer than in control retinas (Fig. 5B). Interestingly, in the *marcksl1b* morphants, some degree of RGC layer disruption was always evident, with groups of differentiating neurons appearing displaced towards the apical (outer) retina. In embryos with an apparently more severe phenotype some RGCs, either isolated or in groups, appeared mislocalized towards the apical side of the retinal neuroepithelium (Fig. 5C). In the case of double *marcksl1a+marckls1b* morphants, the phenotype was similar, albeit more severe regarding the size of the retina and the number of differentiating neurons, both at 35 and 60 hpf (Fig. 5A-B).

As described by Ott and collaborators (Ott et al., 2011), we found that both *marcksa* and *marcksb* MOs also caused an apparent delay in neuronal differentiation and smaller eyes in hypomorphs generated by injecting 0.3 pmol of MO per embryo (Fig. S6, see also Fig. S4). A significant difference was found, however at higher doses of each MO (≥0.4 pmol). While for *marcksa* only an accentuation of the delayed differentiation phenotype was observed (not shown), important malformations, characterized by a complete loss of retinal layers and pronounced folding of the retinal wall, were seen in the case of *marcksb* (Fig. 6A and B, see also Fig. S4). By injecting Atoh7:Gap43-EGFP ("Atoh7") transgenic embryos with *marcksb* MO, later stained for F-Actin and nuclei, an ingression of ectopic F-Actin accumulations into the retinal wall was evident, causing an alteration in the distribution of differentiating RGCs and their progenitors (Fig. 6B and B'). In particular, the cell bodies appeared to avoid these actin-enriched structures, while some elongated progenitors or neuroblasts were connected to them by their apical processes, indicating the apical neuroepithelial border identity of these actin accumulations (Fig. 6B and B'). Given that coinjection of *marcksb* and *marcksl1a* MOs caused severe disorganization in the hindbrain and spinal cord, we

decided to analyze the phenotype of these double morphants in the retina. Here, again a striking morphogenesis defect was evident, as double morphant retinas appeared more severely folded than in the *marcksb*-alone morphant, to the point that the retinal structure was completely disrupted and an optic cup-shape was no longer evident (Fig. 6B). In most cases, no or very few Atoh7-positive cells were seen at 48 hpf, and when present they appeared disorganized albeit still apparently able to differentiate, as some growing axons could be observed (Fig. 6B''').

marcks genes knockdown and cilia length

Some of the morphological features observed in *marcksl1a* morphant embryos (like reduced eye size, enlarged brain ventricles and a ventrally-curved body) are typically seen when cilia integrity is affected (Sun et al., 2004; Tsujikawa and Malicki, 2004). In addition, we found that in many (26/71) *marcksl1a* morphant embryos, three otoliths were visible instead of two, another morphological hallmark of cilia malfunction (Fig. 7A). Although cilia were not evidently reduced in the inner ear (not shown), acetylated-tubulin-positive cilia were much fewer and shorter in the olfactory placode of *marcksl1a* morphant embryos than in controls (Fig. 7B). To further explore the possibility that *marcksl1a*, or other *marcks* genes, were involved in regulating cilia formation or maintenance, we measured the length of cilia in the Kupffer's vesicle, an organ specialized in the determination of left-right asymmetry and enriched in easy-to-see primary cilia that have been extensively used to study cilia physiology in the zebrafish (Zhao and Malicki, 2007). Remarkably, we found that all four *marcks* MOs, injected individually, caused a significant reduction in cilia length, in the Kupffer's vesicle of 8-10 somites embryos (Fig. 7C-D).

DISCUSSION

Four *marcks* genes in teleosts, and hints on their evolutionary process

In most species in which *marcks* genes have been described, there are two different members of the family, each encoding only one protein (Aderem, 1992): MARCKS and MARCKSL1. Here, we report the existence of two apparently functional genes for MARCKSL1, which added to the previously described genes encoding MARCKS (Ott et al., 2011), results in a total of four different *marcks* family genes being expressed in the zebrafish. The current availability of many complete genome sequences allowed us to perform a relatively broad search for *marcks* family members across different species, leading to some interesting observations. In the first place, we have been able to find recognizable *marcks* genes only in gnathostomes, suggesting a relatively recent appearance of these genes in evolution. Secondly, all teleosts, and only teleosts, appear to have four *marcks* family members, while sarcopterigians and ancient fish just present one *marcks* and one *marcksl1* genes. Even if there is an evident degree of divergence among all MARCKS protein sequences, we observed that most of the suspected orthologs grouped very well after phylogenetic analysis, following the accepted evolutionary pathway in most of the cases. As previously shown for a smaller phylogeny (Ott et al., 2011), zebrafish (and the other teleosts) MARCKSA sequence groups with MARCKS protein sequences from other species, while all the teleosts MARCKSB proteins form an independent group. All MARCKSL1 protein sequences analyzed appeared as highly derived and with greater degrees of divergence among them when comparing different vertebrate classes. Although the comparison at the protein level resulted in a positioning of zebrafish and medaka MARCKSA apart from the rest of the teleost corresponding sequences in the phylogeny, the phylogenetic analysis of the genomic coding sequences as well as the analysis of relative evolution times showed that they both group with the expected orthologs in teleosts, apart from ancient actinopterigians and chondrichtyans.

All these observations strongly support the idea that *marcks* genes were completely duplicated, and maintained, after the third whole genome duplication ("3R") in vertebrates, which only affected teleosts (Glasauer and Neuhauss, 2014). Interestingly, the observation of only four (instead of eight) genes in teleosts, and two (instead of four) in ancient fish and sarcopterigians, suggests that either these genes were not duplicated in (or lost shortly after) one of the two first genome duplications (1R/2R), or that the original ancestor *marcks* gene appeared between them. The fact that we failed to find *marcks* genes in the available agnaths genomes supports the hypothesis of an origin after 1R, as this group may have diverged from the gnathostomes before these duplications (Putnam et al., 2008; Mehta et al., 2013), and situates the possible origin of the ancient *marcks* gene at a period between 477 and 450 mya (Ravi and Venkatesh, 2008). The completion of more genomic sequences from basal vertebrates will eventually allow for the confirmation of this supposition. When protein sequences and their alignments are analyzed in more detail, we can see that, as it has been described for higher vertebrates alone (Li and Aderem, 1992; Blackshear, 1993), the three MARCKS conserved domains can still be recognized. Regarding the MH2, it is interesting that all non-teleost MARCKS and all teleost MARCKSA sequences share the presence of a serine phosphorylatable by Cdk5, homolog to chick S25, whose phosphorylation was previously shown to correlate to neuronal differentiation in chick and mouse embryos (Zolessi et al., 2004; Toledo et al., 2013; Contreras-Vallejos et al., 2014). This serine is not present in any of the identified teleosts MARCKSB protein sequences, or in most MARCKSL1. It is tempting to speculate then, that the presence of an S25-like phosphorylatable residue is an ancient feature that has been lost during evolution in most but *marcks* and *marcksa* genes.

Finally, in spite of these relatively conserved regions, multiple sequence alignment of MARCKS family of proteins among different species clearly show a high degree of divergence in the other areas, particularly the carboxy-terminus half. It has been demonstrated that disordered regions in proteins tend to have a much higher rate of aminoacid exchange than ordered regions in the same proteins (Denning and Rexach, 2007; Brown et al., 2011). It is interesting, however, that most

experimental and theoretical evidence indicates that MARCKS is largely disordered, with probably only very short stretches comprising a few aminoacids containing some secondary structure (Arbuzova et al., 2002; Yamauchi et al., 2003; Tapp et al., 2005; Tinoco et al., 2014). Hence, even the conserved regions in MARCKS might be disordered in the native protein. It has been shown that conserved disordered protein sequences also occur in many other proteins, and that they usually have essential functions such as mediating interactions with other macromolecules (Chen et al., 2006).

Functional diversification of the zebrafish *marcks* genes

That four genes have been maintained, and in addition diverged after genome duplication, suggests they may have acquired different functions during teleost evolution. For the zebrafish *marcks* genes for which there are *in situ* hybridization data (*marcksa*: Thisse and Thisse, 2004; *marcksb*: Wang et al., 2013; *marcksl1a*: Thisse et al., 2001), a widespread distribution from early to late embryonic stages has been shown, with a usually higher expression in the central nervous system. Our quantitative RT-PCR analysis also showed that all four *marcks* genes are expressed along the first three days of development. Only *marcksa* showed some dynamics within this period, with a higher amount of mRNA at 24 hpf, suggesting more important roles during early developmental stages. Previous RNA-seq data from an earlier developmental period (Vesterlund et al., 2011) also revealed higher expression levels of *marcksa* at early stages, reaching a maximum at around 11 hpf. By knocking down zebrafish *marcks* genes, we found that even if all MOs caused phenotypes suggesting a function in neural development, there are very interesting differences between them. Contrary to what was previously reported (Ott et al., 2011), we found that *marcksb*, and not *marcksa*, caused severe morphogenetic defects in both the hindbrain and retina. Similarly, *marcksl1a* MO showed a marked phenotype in brain morphogenesis which was different to that of

marcksb, while *marcksl1b* MO showed a unique phenotype in the retina. Interestingly, some relative differences were evident in the semiquantitative RT-PCR analysis from different adult tissues, which are consistent with some of the functional knockdown data. For example, *marcksl1a* mRNA is more abundant in the central nervous system (particularly the eye) than in skeletal muscle, while *marcksb* has a higher expression in muscle. Malformation of skeletal muscle fibers was described for both *marcksa* and *marcksb* morphants in the zebrafish (Ott et al., 2011), an observation we observed only for *marcksb* (results not shown), and the modulation of MARCKS phosphorylation state has been shown to be essential during skeletal myoblasts spreading, migration and fusion in culture (see for example Kim et al., 2000; Louis et al., 2008).

Defects in cephalic neural tube closure are amongst the major defects that were observed in mice mutant for *marcks* and *marcksl1 (Stumpo et al., 1995; Chen et al., 1996)*. In those experiments, *marcksl1* had a much higher penetrance in its phenotype, indicating slight differences on the functions of these two genes in neurulation. Although the process of neural tube formation, at the morphological level, is remarkably different in teleosts when compared to tetrapods, many pieces of evidence suggest that the essential mechanisms are very similar, both at the cellular and molecular level. Even some morphogenetic steps, such as the formation of hingepoints, appear to be conserved in fish (Nyholm et al., 2009). Interestingly, in the zebrafish we observed that *marcksb* caused a major defect only in the hindbrain, which had a larger ventricle and presented wider wall angles respect to the floorplate, while in *marcksl1a* morphants all ventricles appeared enlarged, and there was a different sort of abnormality in the angle of the hindbrain walls: a “T-shaped” neural plate. Interestingly, a similar shape was described for N-Cadherin mutants (Hong and Brewster, 2006), while a larger hindbrain ventricle like that seen in *marcksb* morphants was observed for Pard3 (Hong et al., 2010). Both N-Cadherin and Pard3 are essential in maintaining the subapical adhesion complexes and regulating neuroepithelial polarity, which is in accordance with the apical localization of MARCKS in the chick neural plate, previously reported by us (Zolessi and Arruti, 2001b). Surprisingly, we observed the appearance of new phenotypical features in double

marcksb+marcksl1a morphants, indicating that both genes interact and are necessary for the correct formation of the neural tube in the zebrafish. The most striking observation was that, in many embryos, parts of the neural tube (particularly from hindbrain to spinal cord) were duplicated. A similar phenotype was previously demonstrated in planar cell polarity (PCP) pathway zebrafish mutants, such as *trilobite* (*vangl2* mutant) (Tawk et al., 2007), as well as in embryos with impaired mesoderm differentiation (Araya et al., 2014). Hence, these two MARCKS proteins (MARCKSB and MARCKSL1A) appear to be modulating both apico-basal and planar cell polarity in zebrafish neurulation. This is not surprising if we take into account the major role of MARCKS proteins in modulating the actin cytoskeleton. The sub-apical actin meshwork is directly connected to the protein complexes modulating apical-basal cell polarity, particularly through its interaction with Cadherin-mediated cell adhesion (Miyamoto et al., 2015). On the other hand, the PCP pathway exerts part of its functions through the modulation of the actin cytoskeleton (Devenport, 2016). Interestingly, MARCKSB was recently shown to be necessary for zebrafish gastrulation (Wang et al., 2013), while MARCKS was indicated as an essential intermediate between cortical actin and the PCP pathway during frog gastrulation, where its knockdown using MOs showed severe defects in convergent extension (Iioka et al., 2004).

In the case of another region of the central nervous system, the retina, major morphogenetic phenotypes were observed only for the knockdown of *marcksb* and *marcksl1b*. *marcksb* morphants showed deformations of the retinal wall reminiscent to the folding observed in some mice mutant for the *marcks* gene (Scarlett and Blackshear, 2003), a phenotype that was extensively exacerbated by the transgenic complementation of this mutation with a form of the protein unable to attach to the plasma membrane (Kim et al., 1998). *marcksl1b* morphants, on the other hand, presented milder distortions affecting the organization of RGCs, some of which eventually appeared apically mislocalized. These retinal malformations could all be related to MARCKS family proteins function in modulating the actin cytoskeleton, an essential structure for the maintenance of neuroepithelial integrity and retinal morphogenesis (Chauhan et al., 2015). Similar, albeit more severe retinal

phenotypes have been described in epithelial polarity zebrafish mutants in which apical complex proteins are affected, such as *nok* (Pals-1), *has* (aPKCλ) or *ome* (Crb2a) (Malicki et al., 1996; Zolessi et al., 2006). Defects in progenitor cells (radial glia) localization, accompanied by a loss in apical proteins localization, were also observed in the differentiating cerebral cortex of mouse *marcks* mutants (Weimer et al., 2009). It is remarkable that the co-injection of *marcksl1a* MO (which seems not to have an effect on its own in the retina) with *marcksb* MO, caused an extremely severe phenotype indicating a collaboration of *marcksl1a*, and that *marcksb* is necessary but not sufficient for regulating the process of retinal morphogenesis. A role for *marcksl1* in promoting retinal progenitors proliferation has been previously reported in mice (Zhao et al., 2007), which is consistent with the observation of reduced cell number and delayed differentiation in all zebrafish *marcks* morphants. Finally, the observed phenotypes in head cartilage formation point to a role of zebrafish MARCKS proteins in neural crest migration and/or differentiation, as was also suggested by the observation that MARCKS is phosphorylated at S25 during neural crest migration in the chick embryo (Ruiz-Perera et al., 2013).

Surprisingly, one feature common to all zebrafish *marcks* genes was their effect on cilia length at the Kupffer's vesicle. Although especially evident in the *marcksl1a* morphant, all of them presented similarities with the well characterized morphologies of zebrafish ciliogenesis mutants like *ift88*, *ift20* or *elipsa* (see for example Tsujikawa and Malicki, 2004). Although no function for MARCKS or MARCKSL1 has been previously demonstrated in relation to cilia formation or maintenance, a centrosomal localization of ED-phosphorylated MARCKS has been reported in mouse eggs (Michaut et al., 2005). Anyhow, an indirect effect of *marcks*-family knockdown could also be responsible for this phenotype. For example, a close functional relationship has been shown between the integrity of Actin filaments and cilia maintenance (Antoniades et al., 2014), suggesting that it might be possible that F-Actin modulation by MARCKS underlies the observed effect. In zebrafish nervous system morphogenesis, a role has been demonstrated for cilia affecting planar cell polarity (Borovina et al., 2010), and interestingly, we found that at least three of the zebrafish

marcks genes (*marcksb*, *marcksl1a* and *marcksl1b*) appear to affect convergent extension during neurulation. Regarding the retina, it was recently shown that experimental cilia impairment causes different defects in the development of this organ, including a preferential delay in RGCs generation and differentiation (Lepanto et al., 2016). Therefore, it would be possible to speculate that most of the nervous system development defects discussed above are actually caused by cilia disfunction. However, the existence of some relevant differences between morphants still argue in favor of an important degree of functional specialization.

Conclusions

In summary, the *marcks* family of genes, with its peculiar characteristics like being very small and highly divergent, appears to be more complex in the zebrafish (and probably in all teleosts) than in mammals, where only two different genes exist. This complexity is reflected in both similarities and differences between phenotypes in development, which indicate some degree of interaction or shared functions, while at the same time, some clearly different activities emerge (see Table S6 for a summary). The MARCKS family could hence become a paradigm for understanding gene functional diversification along evolution, with a special emphasis in developmental processes. Largely unfolded proteins like these do not present the structural constraints that prevent sequence modifications in most other proteins, and may act then as powerful sources for the generation of novel functions.

Acknowledgements: The authors want to thank Cristina Arruti for continuous support and for insightful discussion on the manuscript; Ana Paula Arévalo, Casandra Carrillo and Nicolás Papa for technical assistance on fish maintenance; José Badano for antibodies; Gabriela Casanova for

materials and granting access to the ultramicrotome; Gabriela Libisch for helpful assistance on Q-PCR analysis; Soledad Astrada, Marcela Díaz and Tabaré De Los Campos for technical assistance on confocal microscopy and image processing; Martín Graña for critically reading the manuscript and useful comments. The authors declare no conflict of interest.

LITERATURE CITED

Aderem A. 1992. The MARCKS brothers: a family of protein kinase C substrates. Cell 71:713–6.

Altschul SF, Gish W, Miller W, Myers EW, Lipman DJ. 1990. Basic local alignment search tool. J Mol Biol 215:403–10.

Antoniades I, Stylianou P, Skourides P. 2014. Making the Connection: Ciliary Adhesion Complexes Anchor Basal Bodies to the Actin Cytoskeleton. Dev Cell 28:70–80.

Araya C, Tawk M, Girdler GC, Costa M, Carmona-Fontaine C, Clarke JD. 2014. Mesoderm is required for coordinated cell movements within zebrafish neural plate in vivo. Neural Dev 9:9.

Arbuzova A, Schmitz AAP, Vergères G. 2002. Cross-talk unfolded: MARCKS proteins. Biochem J 362:1–12.

Blackshear PJ. 1993. The MARCKS family of cellular protein kinase C substrates. J Biol Chem 268:1501–4.

Borovina A, Superina S, Voskas D, Ciruna B. 2010. Vangl2 directs the posterior tilting and asymmetric localization of motile primary cilia. Nat Cell Biol 12:407–12.

Brown CJ, Johnson AK, Dunker a. K, Daughdrill GW. 2011. Evolution and disorder. Curr Opin Struct Biol 21:441–6.

Chauhan B, Plageman T, Lou M, Lang R. 2015. Epithelial morphogenesis: the mouse eye as a model system. Curr Top Dev Biol 111:375–99.

Chen J, Chang S, Duncan SA, Okano HJ, Fishell G, Aderem A. 1996. Disruption of the MacMARCKS gene prevents cranial neural tube closure and results in anencephaly. Proc Natl Acad Sci U S A 93:6275–79.

Chen JW, Romero P, Uversky VN, Dunker AK. 2006. Conservation of intrinsic disorder in protein domains and families: II. functions of conserved disorder. J Proteome Res 5:888–98.

Chevenet F, Brun C, Bañuls A-L, Jacq B, Christen R. 2006. TreeDyn: towards dynamic graphics and annotations for analyses of trees. BMC Bioinformatics 7:439.

Contreras-Vallejos E, Utreras E, Bórquez DA, Prochazkova M, Terse A, Jaffe H, Toledo A, Arruti C, Pant HC, Kulkarni AB, González-Billault C. 2014. Searching for novel Cdk5 substrates in brain by comparative phosphoproteomics of wild type and Cdk5-/- mice. PLoS One 9:e90363.

Denning DP, Rexach MF. 2007. Rapid evolution exposes the boundaries of domain structure and function in natively unfolded FG nucleoporins. Mol Cell Proteomics 6:272–82.

Dereeper A, Guignon V, Blanc G, Audic S, Buffet S, Chevenet F, Dufayard J-F, Guindon S, Lefort V, Lescot M, Claverie J-M, Gascuel O. 2008. Phylogeny.fr: robust phylogenetic analysis for the non-specialist. Nucleic Acids Res 36:W465–9.

Devenport D. 2016. Tissue morphodynamics: Translating planar polarity cues into polarized cell behaviors. Semin Cell Dev Biol, In Press, doi:10.1016/j.semcdb.2016.03.012

Edgar RC. 2004. MUSCLE: multiple sequence alignment with high accuracy and high throughput. Nucleic Acids Res 32:1792–7.

Eisen JS, Smith JC. 2008. Controlling morpholino experiments: don’t stop making antisense.

Development 135:1735–43.

Gentleman RC, Carey VJ, Bates DM, Bolstad B, Dettling M, Dudoit S, Ellis B, Gautier L, Ge Y, Gentry J, Hornik K, Hothorn T, Huber W, Iacus S, Irizarry R, Leisch F, Li C, Maechler M, Rossini AJ, Sawitzki G, Smith C, Smyth G, Tierney L, Yang JYH, Zhang J. 2004. Bioconductor: open software development for computational biology and bioinformatics. Genome Biol 5:R80.

Glasauer SMK, Neuhauss SCF. 2014. Whole-genome duplication in teleost fishes and its evolutionary consequences. Mol Genet Genomics 289:1045–60.

Graff JM, Stumpo DJ, Blackshear PJ. 1989. Molecular cloning, sequence, and expression of a cDNA encoding the chicken myristoylated alanine-rich C kinase substrate (MARCKS). Mol Endocrinol 3:1903–6.

Guindon S, Dufayard J-F, Lefort V, Anisimova M, Hordijk W, Gascuel O. 2010. New algorithms and methods to estimate maximum-likelihood phylogenies: assessing the performance of PhyML 3.0. Syst Biol 59:307–21.

Harlan DM, Graff JM, Stumpo DJ, Eddy RL, Shows TB, Boyle JM, Blackshear PJ. 1991. The human myristoylated alanine-rich C kinase substrate (MARCKS) gene (MACS): Analysis of its gene product, promoter, and chromosomal localization. J Biol Chem 266:14399–405.

Hong E, Brewster R. 2006. N-cadherin is required for the polarized cell behaviors that drive neurulation in the zebrafish. Development 133:3895–3905.

Hong E, Jayachandran P, Brewster Rachel R. 2010. The polarity protein Pard3 is required for centrosome positioning during neurulation. Dev Biol 341:335–345.

Iioka H, Ueno N, Kinoshita N. 2004. Essential role of MARCKS in cortical actin dynamics during

gastrulation movements. J Cell Biol 164:169–174.

Kent WJ. 2002. BLAT--the BLAST-like alignment tool. Genome Res 12:656–64.

Kim HS, Swierczynski SL, Tuttle JS, Lai WS, Blackshear PJ. 1998. Transgenic complementation of MARCKS deficiency with a nonmyristoylatable, pseudo-phosphorylated form of MARCKS: evidence for simultaneous positive and dominant-negative effects on central nervous system development. Dev Biol 200:146–57.

Kim SS, Kim JH, Kim HS, Park DE, Chung CH. 2000. Involvement of the theta-type protein kinase C in translocation of myristoylated alanine-rich C kinase substrate (MARCKS) during myogenesis of chick embryonic myoblasts. Biochem J 347 Pt 1:139–46.

Kumar S, Stecher G, Tamura K. 2016. MEGA7: Molecular Evolutionary Genetics Analysis Version 7.0 for Bigger Datasets. Mol Biol Evol 30:2725-9.

Larkin MA, Blackshields G, Brown NP, Chenna R, McGettigan PA, McWilliam H, Valentin F, Wallace IM, Wilm A, Lopez R, Thompson JD, Gibson TJ, Higgins DG. 2007. Clustal W and Clustal X version 2.0. Bioinformatics 23:2947–48.

Larsen F, Gundersen G, Lopez R, Prydz H. 1992. CpG islands as gene markers in the human genome. Genomics 13:1095–107.

Lawrence M, Huber W, Pagès H, Aboyoun P, Carlson M, Gentleman R, Morgan MT, Carey VJ. 2013. Software for computing and annotating genomic ranges. PLoS Comput Biol 9:e1003118.

Lepanto P, Davison C, Casanova G, Badano JL, Zolessi FR. 2016. Characterization of primary cilia during the differentiation of retinal ganglion cells in the zebrafish. Neural Dev 11:10.

Li J, Aderem A. 1992. MacMARCKS, a novel member of the MARCKS family of protein kinase C

substrates. Cell 70:791–801.

Louis M, Zanou N, Van Schoor M, Gailly P. 2008. TRPC1 regulates skeletal myoblast migration and differentiation. J Cell Sci 121:3951–9.

Malicki J, Neuhauss SC, Schier a F, Solnica-Krezel L, Stemple DL, Stainier DY, Abdelilah S, Zwartkruis F, Rangini Z, Driever W. 1996. Mutations affecting development of the zebrafish retina. Development 123:263–73.

Maurer-Stroh S, Eisenhaber B, Eisenhaber F. 2002. N-terminal N-myristoylation of proteins: prediction of substrate proteins from amino acid sequence. J Mol Biol 317:541–57.

McWilliam H, Li W, Uludag M, Squizzato S, Park YM, Buso N, Cowley AP, Lopez R. 2013. Analysis Tool Web Services from the EMBL-EBI. Nucleic Acids Res 41 (W1): W597-W600.

Mehta TK, Ravi V, Yamasaki S, Lee AP, Lian MM, Tay B-H, Tohari S, Yanai S, Tay A, Brenner S, Venkatesh B. 2013. Evidence for at least six Hox clusters in the Japanese lamprey (Lethenteron japonicum). Proc Natl Acad Sci U S A 110:16044–9.

Michaut MA, Williams CJ, Schultz RM. 2005. Phosphorylated MARCKS: a novel centrosome component that also defines a peripheral subdomain of the cortical actin cap in mouse eggs. Dev Biol 280:26–37.

Miyamoto Y, Sakane F, Hashimoto K. 2015. N-cadherin-based adherens junction regulates the maintenance, proliferation, and differentiation of neural progenitor cells during development. Cell Adh Migr 9:183–92.

Nyholm MK, Abdelilah-Seyfried S, Grinblat Y. 2009. A novel genetic mechanism regulates dorsolateral hinge-point formation during zebrafish cranial neurulation. J Cell Sci 122:2137–48.

Ott LE, Mcdowell ZT, Turner PM, Law JM, Adler KB, Yoder JA, Jones SL. 2011. Two myristoylated alanine-rich C-kinase substrate (MARCKS) paralogs are required for normal development in zebrafish. Anat Rec 294:1511–24.

Ouimet CC, Wang JK, Walaas SI, Albert KA, Greengard P. 1990. Localization of the MARCKS (87 kDa) protein, a major specific substrate for protein kinase C, in rat brain. J Neurosci 10:1683–98.

Panizzi JR, Jessen JR, Drummond IA, Solnica-Krezel L. 2007. New functions for a vertebrate Rho guanine nucleotide exchange factor in ciliated epithelia. Development 134:921–31.

Pfaffl M. 2004. Quantification strategies in real-time PCR. In: Bustin SA, editor. AZ of quantitative PCR. La Jolla: International University Line. p 87–112.

Prieto D, Aparicio G, Morande PE, Zolessi FR. 2014. A fast, low cost, and highly efficient fluorescent DNA labeling method using methyl green. Histochem Cell Biol 142:335–45.

Putnam NH, Butts T, Ferrier DEK, Furlong RF, Hellsten U, Kawashima T, Robinson-Rechavi M, Shoguchi E, Terry A, Yu J-K, Benito-Gutiérrez EL, Dubchak I, Garcia-Fernàndez J, Gibson-Brown JJ, Grigoriev I V, Horton AC, de Jong PJ, Jurka J, Kapitonov V V, Kohara Y, Kuroki Y, Lindquist E, Lucas S, Osoegawa K, Pennacchio LA, Salamov AA, Satou Y, Sauka-Spengler T, Schmutz J, Shin-I T, Toyoda A, Bronner-Fraser M, Fujiyama A, Holland LZ, Holland PWH, Satoh N, Rokhsar DS. 2008. The amphioxus genome and the evolution of the chordate karyotype. Nature 453:1064–71.

Ravi V, Venkatesh B. 2008. Rapidly evolving fish genomes and teleost diversity. Curr Opin Genet Dev 18:544–50.

Reams AB, Roth JR. 2015. Mechanisms of Gene Duplication and Amplification. Cold Spring Harb Perspect Biol 7:a016592.

Robu ME, Larson JD, Nasevicius A, Beiraghi S, Brenner C, Farber S a, Ekker SC. 2007. p53 activation by knockdown technologies. PLoS Genet 3:787–801.

Ruiz-Perera LM, Arruti C, Zolessi FR. 2013. Early phosphorylation of MARCKS at Ser25 in migrating precursor cells and differentiating peripheral neurons. Neurosci Lett 544:5–9.

Scarlett CO, Blackshear PJ. 2003. Neuroanatomical development in the absence of PKC phosphorylation of the myristoylated alanine-rich C-kinase substrate (MARCKS) protein. Dev Brain Res 144:25–42.

Schindelin J, Arganda-Carreras I, Frise E, Kaynig V, Longair M, Pietzsch T, Preibisch S, Rueden C, Saalfeld S, Schmid B, Tinevez J-Y, White DJ, Hartenstein V, Eliceiri K, Tomancak P, Cardona A. 2012. Fiji: an open-source platform for biological-image analysis. Nat Methods 9:676–82.

Schmitt EA, Dowling JE. 1994. Early eye morphogenesis in the zebrafish, Brachydanio rerio. J Comp Neurol 344:532–42.

Seykora JT, Ravetch J V, Aderem A. 1991. Cloning and molecular characterization of the murine macrophage “68-kDa” protein kinase C substrate and its regulation by bacterial lipopolysaccharide. Proc Natl Acad Sci U S A 88:2505–9.

Sievers F, Wilm A, Dineen D, Gibson TJ, Karplus K, Li W, Lopez R, McWilliam H, Remmert M, Söding J, Thompson JD, Higgins DG. 2011. Fast, scalable generation of high-quality protein multiple sequence alignments using Clustal Omega. Mol Syst Biol 7:539.

Solomon KS, Kudoh T, Dawid IB, Fritz A. 2003. Zebrafish foxi1 mediates otic placode formation and jaw development. Development 130:929–40.

Stumpo DJ, Bock CB, Tuttle JS, Blackshear PJ. 1995. MARCKS deficiency in mice leads to

abnormal brain development and perinatal death. Proc Natl Acad Sci U S A 92:944–8.

Stumpo DJ, Eddy RL, Haley LL, Sait S, Shows TB, Lai WS, Young WS, Speer MC, Dehejia A, Polymeropoulos M, Blackshear PJ. 1998. Promoter sequence, expression, and fine chromosomal mapping of the human gene (MLP) encoding the MARCKS-like protein: identification of neighboring and linked polymorphic loci for MLP and MACS and use in the evaluation of human neural tube defects. Genomics 49:253–64.

Sun Z, Amsterdam A, Pazour GJ, Cole DG, Miller MS, Hopkins N. 2004. A genetic screen in zebrafish identifies cilia genes as a principal cause of cystic kidney. Development 131:4085–93.

Tamura K, Battistuzzi FU, Billing-Ross P, Murillo O, Filipski A, Kumar S. 2012. Estimating divergence times in large molecular phylogenies. Proc Natl Acad Sci U S A 109:19333–8.

Tamura K, Nei M. 1993. Estimation of the number of nucleotide substitutions in the control region of mitochondrial DNA in humans and chimpanzees. Mol Biol Evol 10:512–26.

Tamura K, Stecher G, Peterson D, Filipski A, Kumar S. 2013. MEGA6: Molecular Evolutionary Genetics Analysis version 6.0. Mol Biol Evol 30:2725–9.

Tang R, Dodd A, Lai D, McNabb WC, Love DR. 2007. Validation of zebrafish (Danio rerio) reference genes for quantitative real-time RT-PCR normalization. Acta Biochim Biophys Sin (Shanghai) 39:384–90.

Tapp H, Al-Naggar IM, Yarmola EG, Harrison A, Shaw G, Edison AS, Bubb MR. 2005. MARCKS is a natively unfolded protein with an inaccessible actin-binding site: Evidence for long-range intramolecular interactions. J Biol Chem 280:9946–56.

Tawk M, Araya C, Lyons DA, Reugels AM, Girdler GC, Bayley PR, Hyde DR, Tada M, Clarke

JDW. 2007. A mirror-symmetric cell division that orchestrates neuroepithelial morphogenesis. Nature 446:797–800.

Taylor JS, Braasch I, Frickey T, Meyer A, Van de Peer Y. 2003. Genome duplication, a trait shared by 22000 species of ray-finned fish. Genome Res 13:382–90.

Thisse B, Pflumio S, Fürthauer M, Loppin B, Heyer V, Degrave A, Woehl R, Lux A, Steffan T, Charbonnier X, Thisse C. 2001. Expression of the zebrafish genome during embryogenesis. ZFIN Direct Data Submission (http://zfin.org).

Thisse B, Thisse C. 2004. Fast Release Clones: A High Throughput Expression Analysis. ZFIN Direct Data Submission (http://zfin.org).

Tinoco LW, Fraga JL, Anobom CD, Zolessi FR, Obal G, Toledo A, Pritsch O, Arruti C. 2014. Structural characterization of a neuroblast-specific phosphorylated region of MARCKS. Biochim Biophys Acta - Proteins Proteomics 1844:837–49.

Toledo A, Arruti C. 2009. Actin modulation of a MARCKS phosphorylation site located outside the effector domain. Biochem Biophys Res Commun 383:353–7.

Toledo A, Zolessi FR, Arruti C. 2013. A novel effect of MARCKS phosphorylation by activated PKC: The dephosphorylation of its Serine 25 in chick neuroblasts. PLoS One 8:e62863.

Trevarrow B, Marks DL, Kimmel CB. 1990. Organization of hindbrain segments in the zebrafish embryo. Neuron 4:669–79.

Tsujikawa M, Malicki J. 2004. Intraflagellar transport genes are essential for differentiation and survival of vertebrate sensory neurons. Neuron 42:703–16.

Umekage T, Kato K. 1991. A mouse brain cDNA encodes a novel protein with the protein kinase C phosphorylation site domain common to MARCKS. FEBS Lett 286:147–51.

Vesterlund L, Jiao H, Unneberg P, Hovatta O, Kere J. 2011. The zebrafish transcriptome during early development. BMC Dev Biol 11:30.

Wang Y-W, Wei C-Y, Dai H-P, Zhu Z-Y, Sun Y-H. 2013. Subtractive phage display technology identifies zebrafish marcksb that is required for gastrulation. Gene 521:69–77.

Weimer JM, Yokota Y, Stanco A, Stumpo DJ, Blackshear PJ, Anton ES. 2009. MARCKS modulates radial progenitor placement, proliferation and organization in the developing cerebral cortex. Development 136:2965–75.

Yamauchi E, Nakatsu T, Matsubara M, Kato H, Taniguchi H. 2003. Crystal structure of a MARCKS peptide containing the calmodulin-binding domain in complex with Ca2+-calmodulin. Nat Struct Biol 10:226–31.

Zhao C, Malicki J. 2007. Genetic defects of pronephric cilia in zebrafish. Mech Dev 124:605–16.

Zhao J, Izumi T, Nunomura K, Satoh S, Watanabe S. 2007. MARCKS-like protein, a membrane protein identified for its expression in developing neural retina, plays a role in regulating retinal cell proliferation. Biochem J 408:51–9.

Zolessi FR, Arruti C. 2001a. Sustained phosphorylation of MARCKS in differentiating neurogenic regions during chick embryo development. Dev Brain Res 130:257–67.

Zolessi FR, Arruti C. 2001b. Apical accumulation of MARCKS in neural plate cells during neurulation in the chick embryo. BMC Dev Biol 1:7.

Zolessi FR, Durán R, Engström U, Cerveñansky C, Hellman U, Arruti C. 2004. Identification of the chicken MARCKS phosphorylation site specific for differentiating neurons as Ser 25 using a monoclonal antibody and mass spectrometry. J Proteome Res 3:84–90.

Zolessi FR, Poggi L, Wilkinson CJ, Chien C-B, Harris WA. 2006. Polarization and orientation of

retinal ganglion cells in vivo. Neural Dev 1:2.

FIGURE LEGENDS

FIGURE 1. The *marcks* family of genes in zebrafish and in vertebrates. (A) Intron-exon structure of the four zebrafish *marck*s family members. (B) Phylogenetic relationships among MARCKS family protein sequences in vertebrates. Maximum-likelihood tree showing bootstrap support (percentage) constructed using full-length protein sequences translated from gene and transcript databases (see Table S4 for details). Branches with less than 50% support were collapsed. The *Xenopus tropicalis* MARCKSL1 sequence was used arbitrarily as an external group based on its higher divergence with other MARCKS. Divisions numbered 1-4 depict proteins that we considered to be encoded by ortholog genes (1: *marcks*/*marcksa*; 2: *marcksb*; 3: *marcksl1*/*marcksl1a*; 4: *marcksl1b*).

FIGURE 2. Upstream genomic features and expression of *marcks* family genes in the zebrafish. (A) Upstream CpG-enriched regions in *marcks* family genes in the zebrafish and other vertebrates. Distribution of CpG enrichment regions within the 1 kb upstream region of *marcks* (top) and *marcksl1* (bottom) genes is shown. (B) All four genes are expressed in adult brain, skeletal muscle and whole eye tissues as shown by RT-PCR. DNA ladder references are indicated (base-pairs). (C) Expression levels of *marcks* family genes in the zebrafish, as measured by qRT-PCR. *marcksa* mRNA abundance decays during developmental stages from pharyngula (24 hpf) to larva (72 hpf). *marcksb* levels remain unchanged and lower than those of the oocyte. *marcksl1a* and *marcksl1b* mRNA levels are stable and 5-8 fold higher than in the oocyte during this period. Sequences for all primers used are detailed in Table S1. ntc, non-template control.

FIGURE 3. External phenotype of *marcksl1* MO-injected embryos and defects in head cartilage

development in all *marcks* family morphants. (A) Gross anatomical features of *marcksl1a* and *marcksl1b* single-morphants (0.4 pmol/embryo), and *marcksl1a+marcksl1b* double-morphant (0.2+0.2 pmol/embryo), at two different developmental stages. All treatments included 0.8 pmol/embryo p53 MO, and controls were 0.4 pmol/embryo standard control MO + p53 MO. To better evidence general structure, all embryos were treated with PTU to prevent melanin formation. Arrowheads, dilated fourth ventricle in *marcksb* morphant (B) Alcian blue cartilage staining of *marcks* family single-morphants and *marcksl1a+marcksl1b* double-morphant, indicating their ceratohyal cartilage angle respect to midline. (C) Quantification of ceratohyal angle respect to midline (mean±SEM; n=6 embryos for each treatment) of embryos treated like in (B). (D) Schematic representation of the main head cartilages analyzed. bh, basihyal cartilage; ch, ceratohyal cartilage (red in online color version); hs, hyosymplectic cartilage; M, Meckel's cartilage; pq, palatoquadrate cartilage. Scale bars: A, 350 µm; B, 200 µm.

FIGURE 4. Different but synergistic functions of *marcksb* and *marckls1a* in neural tube morphogenesis. (A) Box-plot representing the angles of the hindbrain walls at the medial hingepoint (MHP) for all *marcks* single morphants and double *marcksb+marcksl1a* morphants, at the same MO doses as in Figure 3. Asterisks: angles significantly different to control with $p<0.05$ (Student's *t* test). Numbers of embryos measured: control, 40; *marcksa* MO, 8; *marcksb* MO, 15; *marcksl1a* MO, 17; *marcksl1b* MO, 5; *marcksb+marcksl1a* MO, 13. (B) Relative frequency distribution of angles at the hindbrain MHP, comparing *marcksb* knockdown and control situation. (C) Transverse optical sections generated by reslicing confocal stacks originally imaged from dorsal to ventral, of zebrafish embryos at 24 hpf treated with MOs to *marcksb* and *marcksl1a* as indicated. F-actin was labeled with TRITC-phalloidin to highlight tissue organization (in the online color version, a nuclear labeling with methyl green is also shown). Dashed lines, examples of angles measured to obtain graphs in A and B; arrowheads, ectopic actin accumulations inside the neuroepithelium in *marcksb+marcksl1a* double morphant; arrow, cells ectopically accumulated in *marcksl1a* morphant.

(D) Resliced optical sections generated and labeled like in C, of 48 hpf embryos treated with *marcksb* and *marcksl1a* MOs. Drawings on the right represent the neural tube section in each confocal image, where the black outer line represents the basal side of the neuroepithelium and the red inner lines represent apical borders, or apical-like F-Actin accumulations (dark gray in the print version). Arrowheads, ectopic F-Actin accumulations inside the neuroepithelium; asterisks, neural tube lumen, completely duplicated in *marcksb+marcksl1a* double morphant. (E) Schematic drawing of the head of a 24 hpf embryo, where straight lines indicate the approximate position of the optical sections shown in the figure. mb, midbrain; ahb, anterior hindbrain; phb, posterior hindbrain. (F) Resliced optical sections through the hindbrain at 24 hpf, of *marcksl1a* and *marcksl1b* MO-injected embryos. These embryos were labeled with an anti-aPKC antibody and TRITC-phalloidin, to highlight apical structures (arrowheads). Drawings on the right represent the neural tube section in each confocal image, where the black outer line represents the basal side of the neuroepithelium and the red inner lines represent apical borders, or apical-like F-Actin accumulations (dark gray in the print version). Scale bars: C and D, 50 µm; F, 30 µm.

FIGURE 5. Effect of *marcksl1* genes knockdown on retinal differentiation and morphogenesis. (A) Confocal sections through the retina of representative 35 hpf *marcksl1a* and *marcksl1b* morphants as indicated. Arrowheads, examples of nuclei with abnormal angles respect to the neuroepithelium in morphants. (B) Confocal sections through the retina of representative 60 hpf *marcksl1a* and *marcksl1b* morphants as indicated. Asterisk, GCL expanded apically in *marcksl1b* morphant. (C) Confocal section through the retina of a different 60 hpf *marcksl1b* morphant at higher magnification to show an ectopic RGC (arrow). Doses of MO are like in Figure 3. RGCs labeled with zn-5 antibody (green in the online color version); F-Actin labeled with TRITC-phalloidin (magenta in the online color version); DNA with methyl green (cyan in the online color version). Ap, apical; Ba, basal; GCL, ganglion cell layer; INL, inner nuclear layer; IPL, inner plexiform layer; L, lens; ONL, outer nuclear layer; OPL, outer plexiform layer. Scale bars: A and B, 30 µm;

C, 10 μm.

FIGURE 6. Effect of the combined *marcksb* and *marcksl1a* knockdown on retinal differentiation and morphogenesis. (A) Semi-thin sections of 48 hpf control and *marcksb* MO-injected embryos, stained with methylene blue. (B) Confocal sections through the eye of 48 hpf *marcksb* and *marcksl1a* morphants as indicated. Squared areas correspond to magnified images in B' and B''. The neural retina extension is marked by a dashed line in the lower right panel (double morphant). (B') Higher magnification of the *marcksb* morphant retina section squared in B, showing retinal ganglion cells (RGC) organization. Arrowheads, RGC neuroblasts or progenitors apical processes contacting the apical-like F-Actin ectopic accumulation; asterisk, area of the neural retina below the F-Actin ectopic accumulation, devoid of Atoh7-positive cells. (B'') Maximum intensity projection of the whole confocal stack of the retina from *marcksb*+*marcksl1a* double morphants (at the area squared in B), showing RGCs organization. Arrows, growing RGC axons. Retinal ganglion cells and progenitors transgenically labeled with Atoh7:Gap43-EGFP (Atoh7); F-Actin labeled with TRITC-phalloidin; DNA labeled with methyl green. Doses of MO are like in Figure 3. Ap, apical retinal neuroepithelium; Ba, basal retinal neuroepithelium; GCL, ganglion cell layer; INL, inner nuclear layer; IPL, inner plexiform layer; L, lens; NR, neural retina; ONL, outer nuclear layer. Scale bars: A, 30 μm; B, 40 μm; B' and B'', 20 μm.

FIGURE 7. Effect of *marcks* genes knockdown on cilia length. (A) Bright-field images of the inner ear of control and *marcksl1a*-MO injected embryos at 48 hpf, showing the otoliths (arrows). (B) Confocal sections through the olfactory pit of control and *marcksl1a*-MO injected embryos at 60 hpf, showing cilia (arrowheads). Cilia labeled with an anti-acetylated tubulin (Ac. Tub.) antibody; F-Actin labeled with TRITC-phalloidin; DNA labeled with methyl green. OE, olfactory epithelium; NR, neural retina. (C) Box-plot showing the effect of *marcks*-family genes knockdown on Kupffer's vesicle cilia length. All morphant embryos have cilia significantly shorter than control at

p<0.0001 (Student's *t* test). Numbers of cilia measured: control, 1575 (52 embryos); *marcksa* MO, 304 (11 embryos); *marcksb* MO, 289 (11 embryos); *marcksl1a* MO, 1405 (34 embryos); *marcksl1b* MO, 1485 (29 embryos). (D) Example confocal sections through Kupffer's vesicle (dashed line) from 10-somite embryos, showing the effect of *marcks*-family genes knockdown on cilia. Cilia labeled with an anti-acetylated tubulin (AcTub) antibody; and, in the online color version, centrosomes labeled with an anti-gamma tubulin (γTub) antibody. Doses of MO are like in Figure 3. Scale bars: A, 25 µm; B, 15 µm; D, 25 µm.

TABLES

TABLE 1. Structure of zebrafish *marcks* gene family.

LEGENDS FOR SUPPLEMENTARY DATA

FIGURE S1. Multiple sequence alignment of MARCKS family proteins from zebrafish. Known functional conserved domains -myristoylation site domain (Myr), MARCKS Homology 2 Domain (MH2) and Effector Domain (ED)- and Clustal consensus are indicated. The serine potentially phosphorylatable by Cdk5, corresponding to chicken MARCKS S25, is highlighted in yellow and only present in zebrafish MARCKSA in position S24 (after excluding the initial M).

FIGURE S2. Multiple sequence alignment of MARCKSL1 proteins from selected species of vertebrates. Known functional conserved domains -myristoylation site domain (Myr), MARCKS Homology 2 Domain (MH2) and Effector Domain (ED)- are indicated. Only the human and coelacanth protein sequences (in addition to the elephant shark sequence, not shown here; see Table

S4), present a serine in a consensus sequence phosphorylatable by Cdk5 (S/T-P-X-K, serine highlighted in yellow), homologous to chicken MARCKS S25.

FIGURE S3. Phylogenetic analysis of *marcks*/*marcksa* genes. (A) Molecular Phylogenetic analysis of *marcks* and *marcksa* genomic coding sequences from fish taxa. The evolutionary history was inferred by using the Maximum Likelihood method based on the Tamura-Nei model. The tree with the highest log likelihood (-2370.7604) is shown. The percentage of trees in which the associated taxa clustered together is shown next to the branches. Initial tree(s) for the heuristic search were obtained automatically by applying Neighbor-Join and BioNJ algorithms to a matrix of pairwise distances estimated using the Maximum Composite Likelihood (MCL) approach, and then selecting the topology with superior log likelihood value. A discrete Gamma distribution was used to model evolutionary rate differences among sites (5 categories [+G, parameter = 0.5649]). (B) Time tree analysis of *marcks* and *marcksa*. A time tree was inferred using the RelTime method and the Tamura-Nei model. The estimated log likelihood value is -2365.8949. A discrete Gamma distribution was used to model evolutionary rate differences among sites (5 categories [+G, parameter = 0.4573]). In Both (A) and (B), the analysis involved 11 nucleotide sequences, where the human *marcks* gene was used as outgroup. Codon positions included were 1st+2nd+3rd+Noncoding. All positions containing gaps and missing data were eliminated. There were a total of 331 positions in the final dataset.

FIGURE S4. Differences in external phenotype of zebrafish embryos treated with MOs against *marcksa* and *marcksb*. (A) 48 hpf embryos injected with control (0.6 pmol), *marcksa* (0.3 pmol) and *marcksb* (0.6 pmol) MOs. Cephalic region of the *marcksb* MO injected embryo shows fourth ventricle oedema (arrowheads) and optic cup malformations. Inset: more evident eye malformations in *marcksb* morphant at 35 hpf. (B) 72 hpf embryos injected with the same MO doses as in A. (C) 48 hpf embryos injected with *marcksb* MO (0.6 pmol, left panel), and coinjected with synthetic

marcksb mRNA (11 fmol). Scale bars: A and inset, 50 µm; B, 150 µm; C, 300 µm.

FIGURE S5. *marcksl1a* mRNA down-regulation by the splice-blocking MO. (A) Microinjection of *marcksl1a* splicing MO elicits phenotypes with different degrees of severity at low (0.16 pmol/embryo; marcksl1a MO +) and high (0.32 pmol/embryo; marcksl1a MO ++) doses at 48 hpf, while no visible phenotype is present in uninjected controls (Control) or embryos injected with control+p53 MOs at the same doses (p53 MO). (B) RT-PCR amplification of *marcksl1a* mRNA from uninjected embryos (-) and embryos injected with different amounts of *marcksl1a* MO (0.2 pmol/embryo, +; 0.4 pmol/embryo, ++). Elongation Factor 1a mRNA (*ef1a*) amplification was used as a PCR control. Details of primer sequences can be found in Table S1. (C) Coinjection of *marcksl1a* mRNA along with *marcksl1a* MO (0.2 pmol) rescues the morphant phenotype in 48 hpf embryos. Scale bars: 300 µm.

FIGURE S6. Confocal sections through the retina of 72 hpf control, *marcksa* or *marcksb*-MO injected embryos, in hypomorphic conditions (0.3 pmol/embryo). (A) Effect on the differentiation of retinal ganglion cells (RGC). (B) Effect on the differentiation of double cone photoreceptors (DC). RGCs labeled with zn-5 antibody; DCs labeled with zpr-1 antibody; F-Actin labeled with TRITC-phalloidin. GCL, ganglion cell layer; INL, inner nuclear layer; IPL, inner plexiform layer; L, lens; ONL, outer nuclear layer; OPL, outer plexiform layer. Scale bar: 30 µm.

TABLE S1. Oligonucleotides and morpholino oligomers used in this work.

TABLE S2. Sequence conservation of *marcks*-family genes.

TABLE S3. Phosphorylation probability of zebrafish MARCKS and MARCKSL1 proteins.

TABLE S4. Accession numbers and details of the sequences used for phylogenetic analysis of MARCKS family proteins.

TABLE S5. Genomic sequences of *marcks*/*marcksa* genes used for phylogenetic analysis.

TABLE S6. Summary of morphant phenotypes and predicted gene and protein features for zebrafish *marcks* family.

VIDEO S1. Animation of resliced confocal stacks from 24 hpf zebrafish embryos injected with MOs to *marcks* genes as indicated. Reconstructed transverse sections span the embryo central nervous system from caudal midbrain to caudal hindbrain. Magenta, TRITC-phalloidin to label F-Actin; green, methyl green to label DNA. Also see Figure 5C.

VIDEO S2. Animation of resliced confocal stacks from 48 hpf zebrafish embryos injected with MOs to *marcks* genes as indicated. Reconstructed transverse sections span the embryo central nervous system from caudal midbrain to caudal hindbrain. Magenta, TRITC-phalloidin to label F-Actin; green, methyl green to label DNA. Also see Figure 5D.

VIDEO S3. Animation of resliced confocal stacks from a 24 hpf zebrafish embryo injected with *marcksl1a* MO. Reconstructed transverse sections span the embryo central nervous system from caudal midbrain to caudal hindbrain. Magenta, TRITC-phalloidin to label F-Actin; green, anti-aPKC antibody; blue, methyl green to label DNA. Also see Figure 5F.

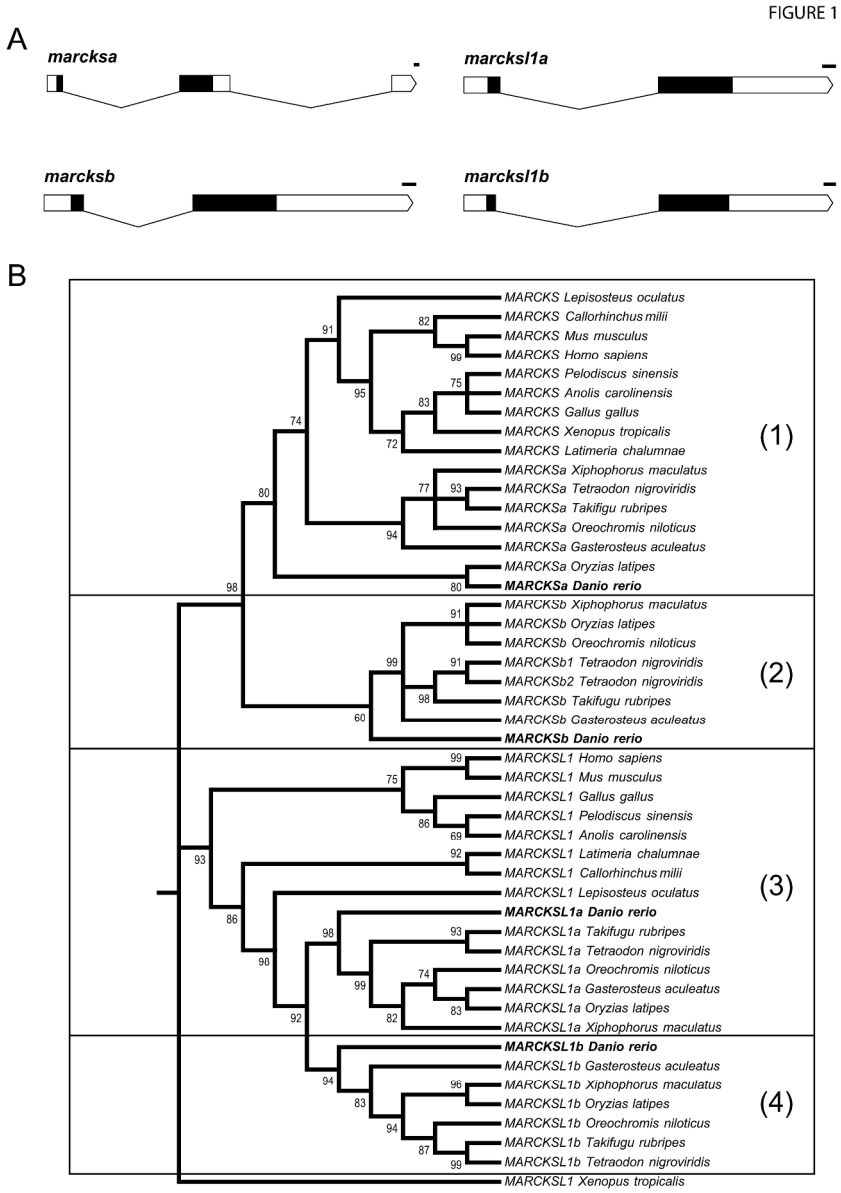

FIGURE 1. The marcks family of genes in zebrafish and in vertebrates. (A) Intron-exon structure of the four zebrafish marcks family members. (B) Phylogenetic relationships among MARCKS family protein sequences in vertebrates. Maximum-likelihood tree showing bootstrap support (percentage) constructed using full-length protein sequences translated from gene and transcript databases (see Table S4 for details). Branches with less than 50% support were collapsed. The Xenopus tropicalis MARCKSL1 sequence was used arbitrarily as an external group based on its higher divergence with other MARCKS. Divisions numbered 1-4 depict proteins that we considered to be encoded by ortholog genes (1: marcks/marcksa; 2: marcksb; 3: marcksl1/marcksl1a; 4: marcksl1b).
271x367mm (300 x 300 DPI)

FIGURE 2

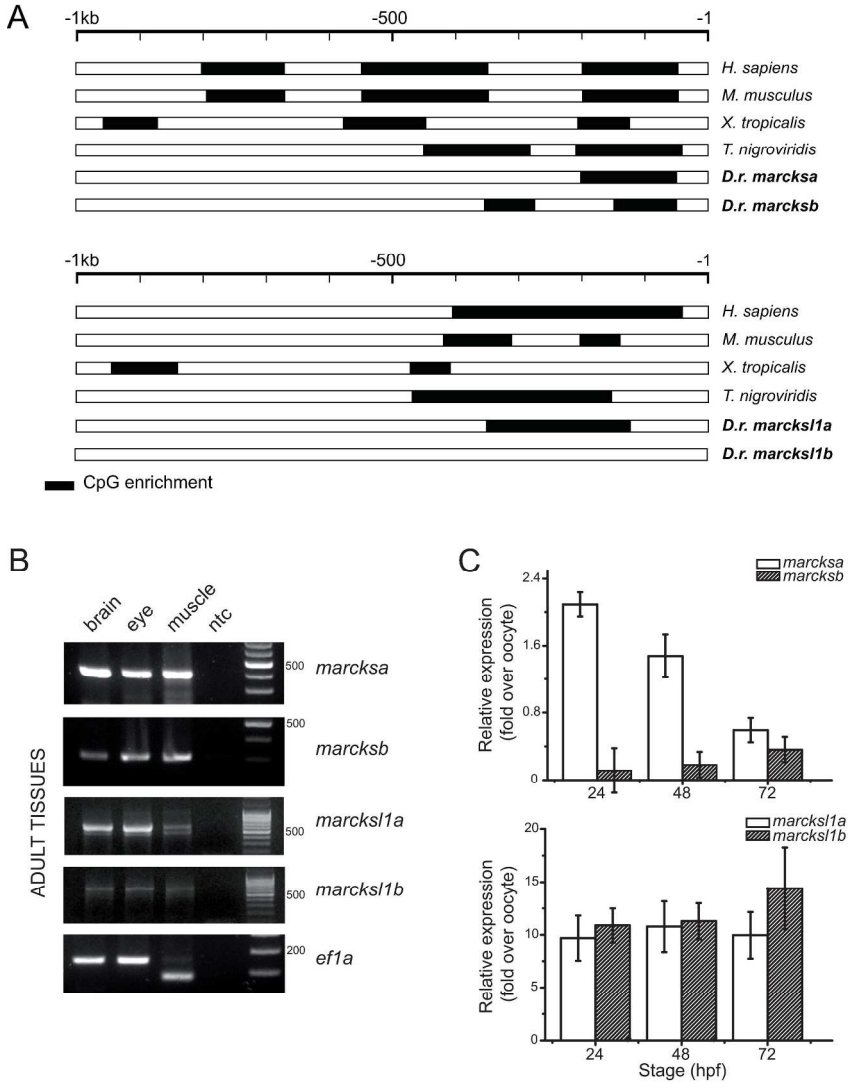

FIGURE 2. Upstream genomic features and expression of marcks family genes in the zebrafish. (A) Upstream CpG-enriched regions in marcks family genes in the zebrafish and other vertebrates. Distribution of CpG enrichment regions within the 1 kb upstream region of marcks (top) and marcksl1 (bottom) genes is shown. (B) All four genes are expressed in adult brain, skeletal muscle and whole eye tissues as shown by RT-PCR. DNA ladder references are indicated (base-pairs). (C) Expression levels of marcks family genes in the zebrafish, as measured by qRT-PCR. marcksa mRNA abundance decays during developmental stages from pharyngula (24 hpf) to larva (72 hpf). marcksb levels remain unchanged and lower than those of the oocyte. marcksl1a and marcksl1b mRNA levels are stable and 5-8 fold higher than in the oocyte during this period. Sequences for all primers used are detailed in Table S1. ntc, non-template control.
253x293mm (300 x 300 DPI)

FIGURE 3 PRINT VERSION

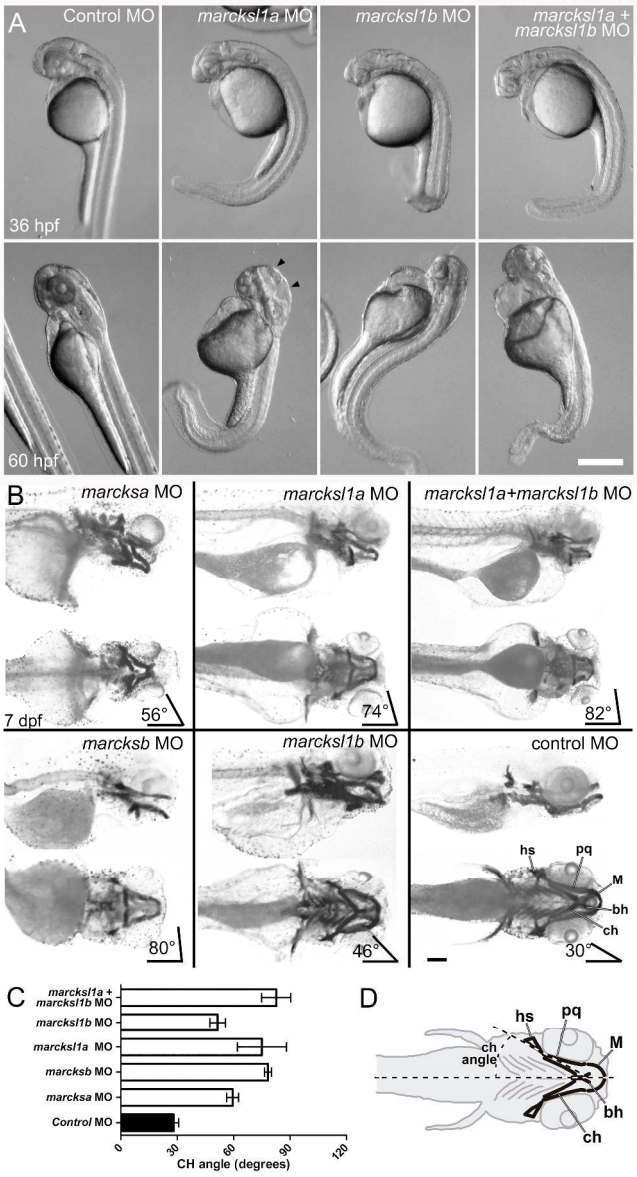

FIGURE 3. External phenotype of marcksl1 MO-injected embryos and defects in head cartilage development in all marcks family morphants. (A) Gross anatomical features of marcksl1a and marcksl1b single-morphants (0.4 pmol/embryo), and marcksl1a+marcksl1b double-morphant (0.2+0.2 pmol/embryo), at two different developmental stages. All treatments included 0.8 pmol/embryo p53 MO, and controls were 0.4 pmol/embryo standard control MO + p53 MO. To better evidence general structure, all embryos were treated with PTU to prevent melanin formation. Arrowheads, dilated fourth ventricle in marcksb morphant (B) Alcian blue cartilage staining of marcks family single-morphants and marcksl1a+marcksl1b double-morphant, indicating their ceratohyal cartilage angle respect to midline. (C) Quantification of ceratohyal angle respect to midline (mean±SEM; n=6 embryos for each treatment) of embryos treated like in (B). (D) Schematic representation of the main head cartilages analyzed. bh, basihyal cartilage; ch, ceratohyal cartilage (red in online color version); hs, hyosymplectic cartilage; M, Meckel's cartilage; pq, palatoquadrate cartilage. Scale bars: A, 350 µm; B, 200 µm.
282x519mm (300 x 300 DPI)

FIGURE 3 ONLINE VERSION

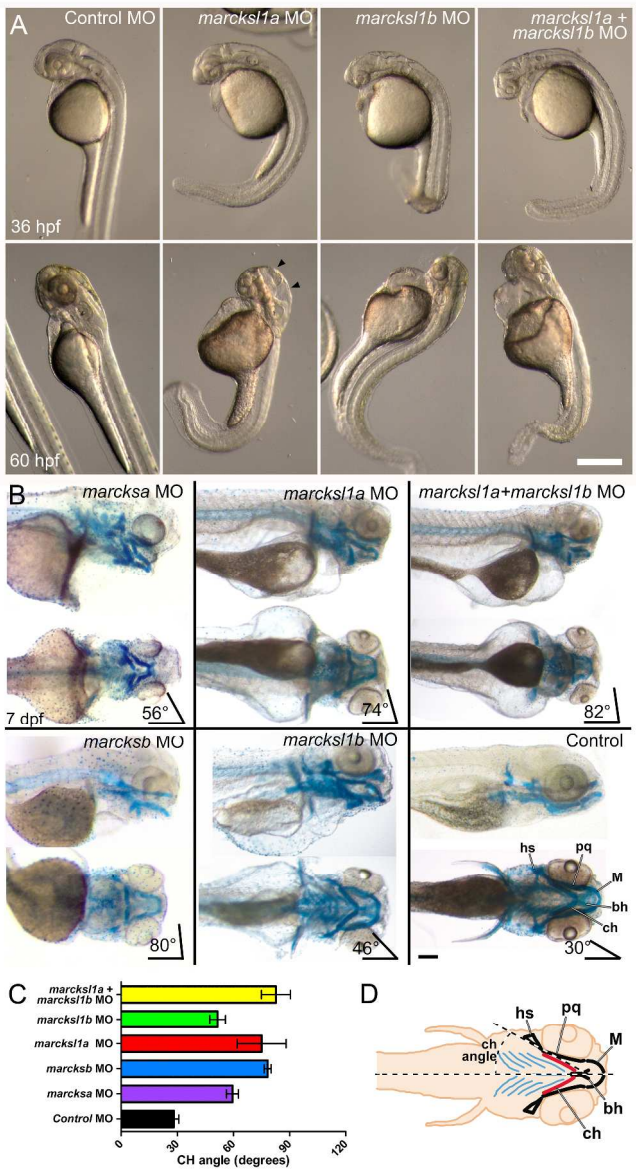

FIGURE 3. External phenotype of marcksl1 MO-injected embryos and defects in head cartilage development in all marcks family morphants. (A) Gross anatomical features of marcksl1a and marcksl1b single-morphants (0.4 pmol/embryo), and marcksl1a+marcksl1b double-morphant (0.2+0.2 pmol/embryo), at two different developmental stages. All treatments included 0.8 pmol/embryo p53 MO, and controls were 0.4 pmol/embryo standard control MO + p53 MO. To better evidence general structure, all embryos were treated with PTU to prevent melanin formation. Arrowheads, dilated fourth ventricle in marcksb morphant (B) Alcian blue cartilage staining of marcks family single-morphants and marcksl1a+marcksl1b double-morphant, indicating their ceratohyal cartilage angle respect to midline. (C) Quantification of ceratohyal angle respect to midline (mean±SEM; n=6 embryos for each treatment) of embryos treated like in (B). (D) Schematic representation of the main head cartilages analyzed. bh, basihyal cartilage; ch, ceratohyal cartilage (red in online color version); hs, hyosymplectic cartilage; M, Meckel's cartilage; pq, palatoquadrate cartilage. Scale bars: A, 350 µm; B, 200 µm.
284x525mm (300 x 300 DPI)

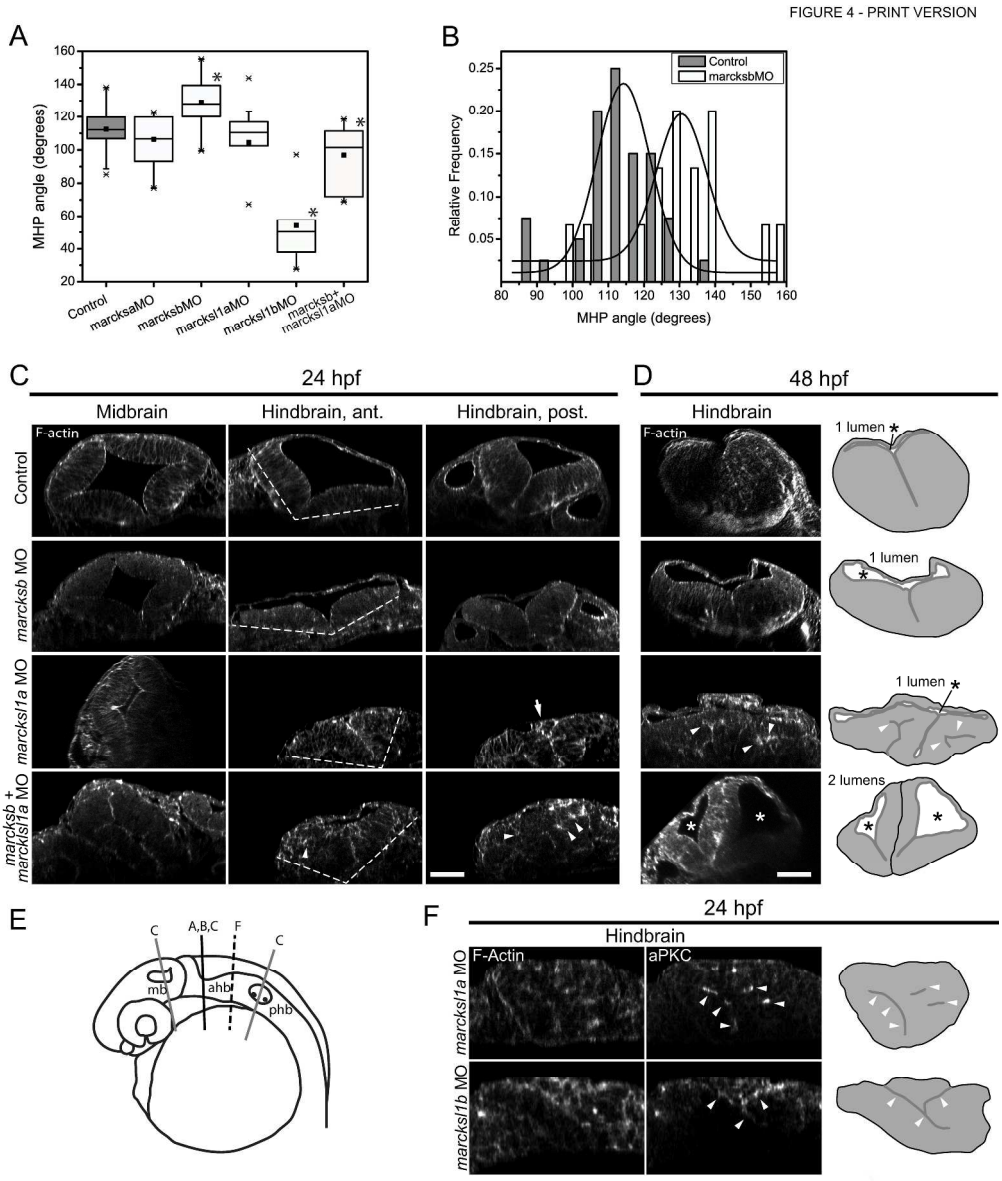

FIGURE 4. Different but synergistic functions of marcksb and marckls1a in neural tube morphogenesis. (A) Box-plot representing the angles of the hindbrain walls at the medial hingepoint (MHP) for all marcks single morphants and double marcksb+marcksl1a morphants, at the same MO doses as in Figure 3. Asterisks: angles significantly different to control with $p<0.05$ (Student's t test). Numbers of embryos measured: control, 40; marcksa MO, 8; marcksb MO, 15; marcksl1a MO, 17; marcksl1b MO, 5; marcksb+marcksl1a MO, 13. (B) Relative frequency distribution of angles at the hindbrain MHP, comparing marcksb knockdown and control situation. (C) Transverse optical sections generated by reslicing confocal stacks originally imaged from dorsal to ventral, of zebrafish embryos at 24 hpf treated with MOs to marcksb and marcksl1a as indicated. F-actin was labeled with TRITC-phalloidin to highlight tissue organization (in the online color version, a nuclear labeling with methyl green is also shown). Dashed lines, examples of angles measured to obtain graphs in A and B; arrowheads, ectopic actin accumulations inside the neuroepithelium in marcksb+marcksl1a double morphant; arrow, cells ectopically accumulated in marcksl1a morphant. (D) Resliced optical sections generated and labeled like in C, of 48 hpf embryos treated with marcksb and marcksl1a MOs. Drawings on the right represent the neural tube section in each confocal image, where the

black outer line represents the basal side of the neuroepithelium and the red inner lines represent apical borders, or apical-like F-Actin accumulations (dark gray in the print version). Arrowheads, ectopic F-Actin accumulations inside the neuroepithelium; asterisks, neural tube lumen, completely duplicated in marcksb+marcksl1a double morphant. (E) Schematic drawing of the head of a 24 hpf embryo, where straight lines indicate the approximate position of the optical sections shown in the figure. mb, midbrain; ahb, anterior hindbrain; phb, posterior hindbrain. (F) Resliced optical sections through the hindbrain at 24 hpf, of marcksl1a and marcksl1b MO-injected embryos. These embryos were labeled with an anti-aPKC antibody and TRITC-phalloidin, to highlight apical structures (arrowheads). Drawings on the right represent the neural tube section in each confocal image, where the black outer line represents the basal side of the neuroepithelium and the red inner lines represent apical borders, or apical-like F-Actin accumulations (dark gray in the print version). Scale bars: C and D, 50 μm; F, 30 μm.
353x414mm (300 x 300 DPI)

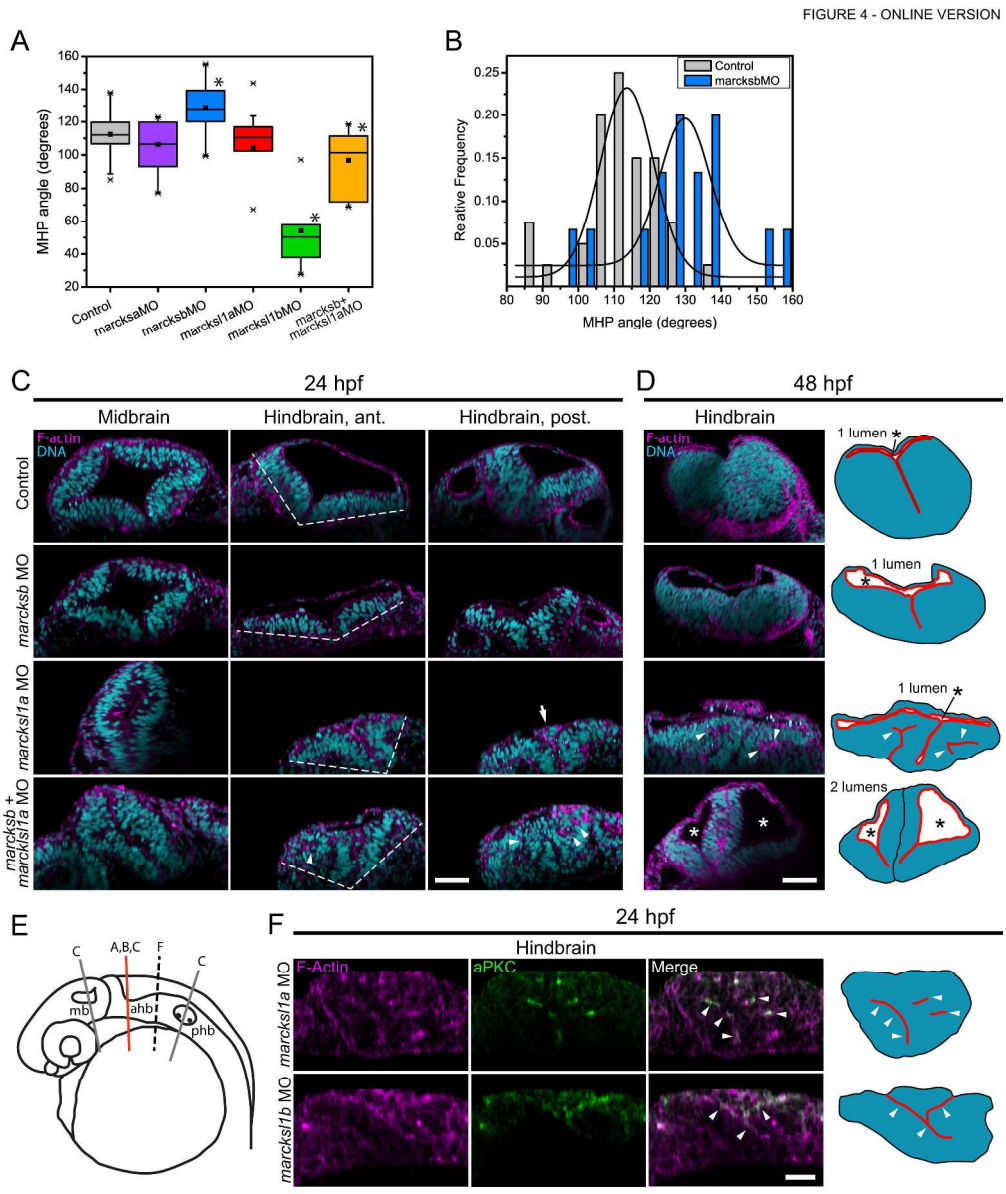

FIGURE 4. Different but synergistic functions of marcksb and marckls1a in neural tube morphogenesis. (A) Box-plot representing the angles of the hindbrain walls at the medial hingepoint (MHP) for all marcks single morphants and double marcksb+marcksl1a morphants, at the same MO doses as in Figure 3. Asterisks: angles significantly different to control with $p<0.05$ (Student's t test). Numbers of embryos measured: control, 40; marcksa MO, 8; marcksb MO, 15; marcksl1a MO, 17; marcksl1b MO, 5; marcksb+marcksl1a MO, 13. (B) Relative frequency distribution of angles at the hindbrain MHP, comparing marcksb knockdown and control situation. (C) Transverse optical sections generated by reslicing confocal stacks originally imaged from dorsal to ventral, of zebrafish embryos at 24 hpf treated with MOs to marcksb and marcksl1a as indicated. F-actin was labeled with TRITC-phalloidin to highlight tissue organization (in the online color version, a nuclear labeling with methyl green is also shown). Dashed lines, examples of angles measured to obtain graphs in A and B; arrowheads, ectopic actin accumulations inside the neuroepithelium in marcksb+marcksl1a double morphant; arrow, cells ectopically accumulated in marcksl1a morphant. (D) Resliced optical sections generated and labeled like in C, of 48 hpf embryos treated with marcksb and marcksl1a MOs. Drawings on the right represent the neural tube section in each confocal image, where the

black outer line represents the basal side of the neuroepithelium and the red inner lines represent apical borders, or apical-like F-Actin accumulations (dark gray in the print version). Arrowheads, ectopic F-Actin accumulations inside the neuroepithelium; asterisks, neural tube lumen, completely duplicated in marcksb+marcksl1a double morphant. (E) Schematic drawing of the head of a 24 hpf embryo, where straight lines indicate the approximate position of the optical sections shown in the figure. mb, midbrain; ahb, anterior hindbrain; phb, posterior hindbrain. (F) Resliced optical sections through the hindbrain at 24 hpf, of marcksl1a and marcksl1b MO-injected embryos. These embryos were labeled with an anti-aPKC antibody and TRITC-phalloidin, to highlight apical structures (arrowheads). Drawings on the right represent the neural tube section in each confocal image, where the black outer line represents the basal side of the neuroepithelium and the red inner lines represent apical borders, or apical-like F-Actin accumulations (dark gray in the print version). Scale bars: C and D, 50 μm; F, 30 μm.
353x416mm (300 x 300 DPI)

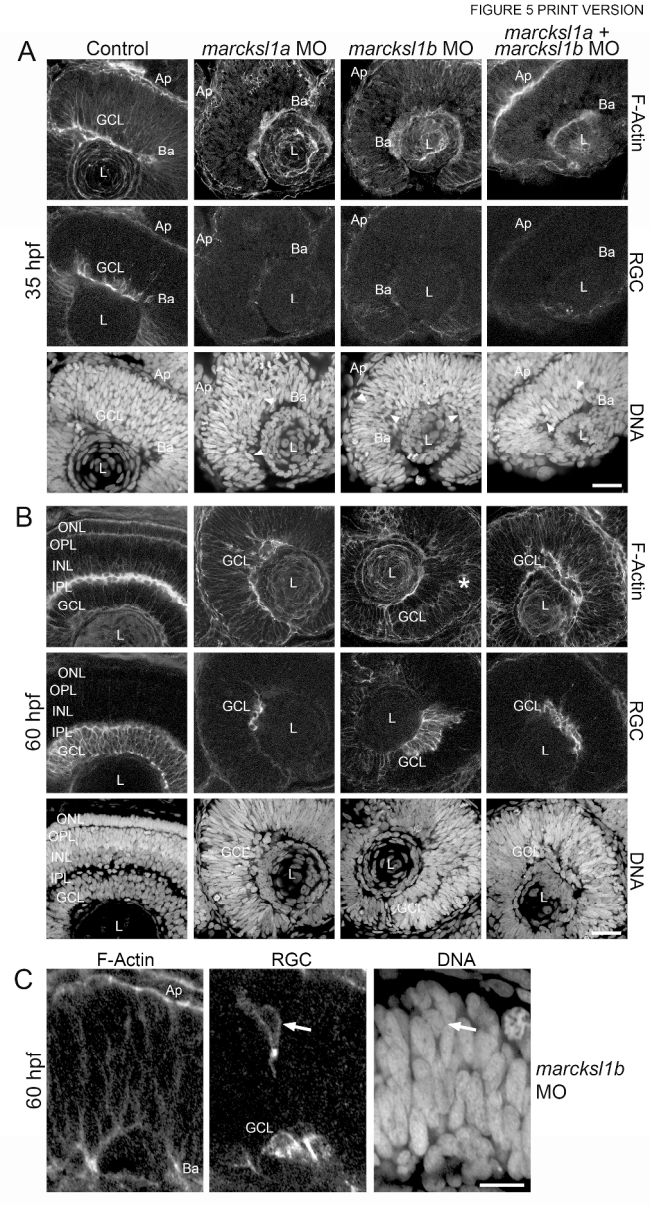

FIGURE 5. Effect of marcksl1 genes knockdown on retinal differentiation and morphogenesis. (A) Confocal sections through the retina of representative 35 hpf marcksl1a and marcksl1b morphants as indicated. Arrowheads, examples of nuclei with abnormal angles respect to the neuroepithelium in morphants. (B) Confocal sections through the retina of representative 60 hpf marcksl1a and marcksl1b morphants as indicated. Asterisk, GCL expanded apically in marcksl1b morphant. (C) Confocal section through the retina of a different 60 hpf marcksl1b morphant at higher magnification to show an ectopic RGC (arrow). Doses of MO are like in Figure 3. RGCs labeled with zn-5 antibody (green in the online color version); F-Actin labeled with TRITC-phalloidin (magenta in the online color version); DNA with methyl green (cyan in the online color version). Ap, apical; Ba, basal; GCL, ganglion cell layer; INL, inner nuclear layer; IPL, inner plexiform layer; L, lens; ONL, outer nuclear layer; OPL, outer plexiform layer. Scale bars: A and B, 30 μm; C, 10 μm.
199x369mm (300 x 300 DPI)

FIGURE 5 ONLINE VERSION

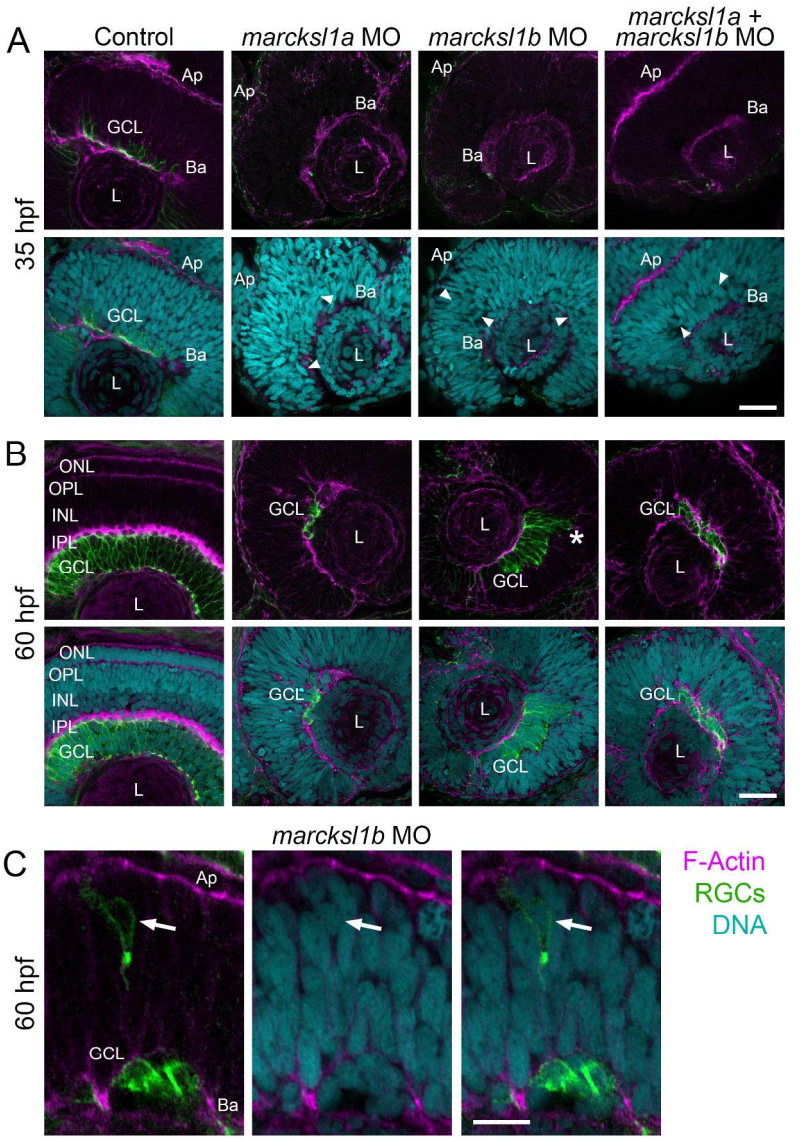

FIGURE 5. Effect of marcksl1 genes knockdown on retinal differentiation and morphogenesis. (A) Confocal sections through the retina of representative 35 hpf marcksl1a and marcksl1b morphants as indicated. Arrowheads, examples of nuclei with abnormal angles respect to the neuroepithelium in morphants. (B) Confocal sections through the retina of representative 60 hpf marcksl1a and marcksl1b morphants as indicated. Asterisk, GCL expanded apically in marcksl1b morphant. (C) Confocal section through the retina of a different 60 hpf marcksl1b morphant at higher magnification to show an ectopic RGC (arrow). Doses of MO are like in Figure 3. RGCs labeled with zn-5 antibody (green in the online color version); F-Actin labeled with TRITC-phalloidin (magenta in the online color version); DNA with methyl green (cyan in the online color version). Ap, apical; Ba, basal; GCL, ganglion cell layer; INL, inner nuclear layer; IPL, inner plexiform layer; L, lens; ONL, outer nuclear layer; OPL, outer plexiform layer. Scale bars: A and B, 30 μm; C, 10 μm.
199x289mm (300 x 300 DPI)

FIGURE 6 PRINT AND ONLINE

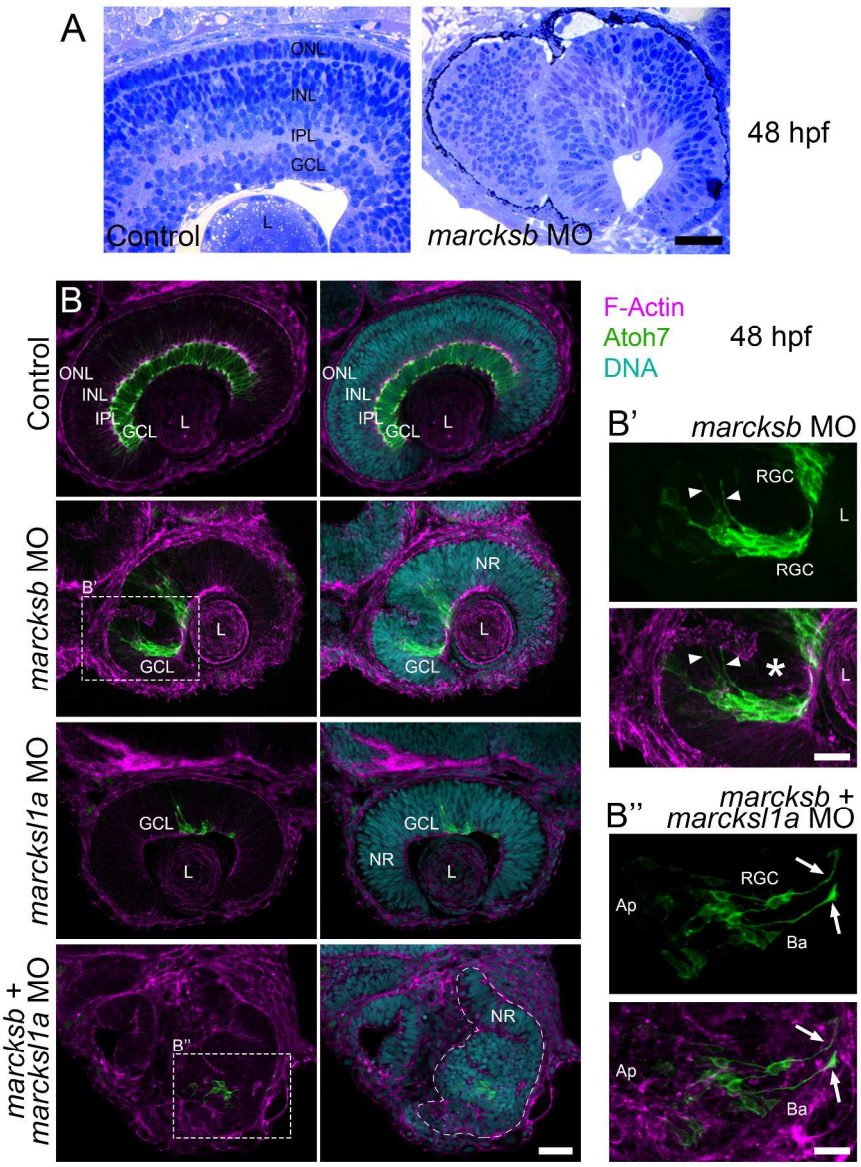

FIGURE 6. Effect of the combined marcksb and marcksl1a knockdown on retinal differentiation and morphogenesis. (A) Semi-thin sections of 48 hpf control and marcksb MO-injected embryos, stained with methylene blue. (B) Confocal sections through the eye of 48 hpf marcksb and marcksl1a morphants as indicated. Squared areas correspond to magnified images in B' and B''. The neural retina extension is marked by a dashed line in the lower right panel (double morphant). (B') Higher magnification of the marcksb morphant retina section squared in B, showing retinal ganglion cells (RGC) organization. Arrowheads, RGC neuroblasts or progenitors apical processes contacting the apical-like F-Actin ectopic accumulation; asterisk, area of the neural retina below the F-Actin ectopic accumulation, devoid of Atoh7-positive cells. (B'') Maximum intensity projection of the whole confocal stack of the retina from marcksb+marcksl1a double morphants (at the area squared in B), showing RGCs organization. Arrows, growing RGC axons. Retinal ganglion cells and progenitors transgenically labeled with Atoh7:Gap43-EGFP (Atoh7); F-Actin labeled with TRITC-phalloidin; DNA labeled with methyl green. mab, marcksb; ml1a, marcksl1a. Doses of MO are like in Figure 3. Ap, apical retinal neuroepithelium; Ba, basal retinal

neuroepithelium; GCL, ganglion cell layer; INL, inner nuclear layer; IPL, inner plexiform layer; L, lens; NR, neural retina; ONL, outer nuclear layer. Scale bars: A, 30 μm; B, 40 μm; B′ and B′′, 20 μm.
249x346mm (300 x 300 DPI)

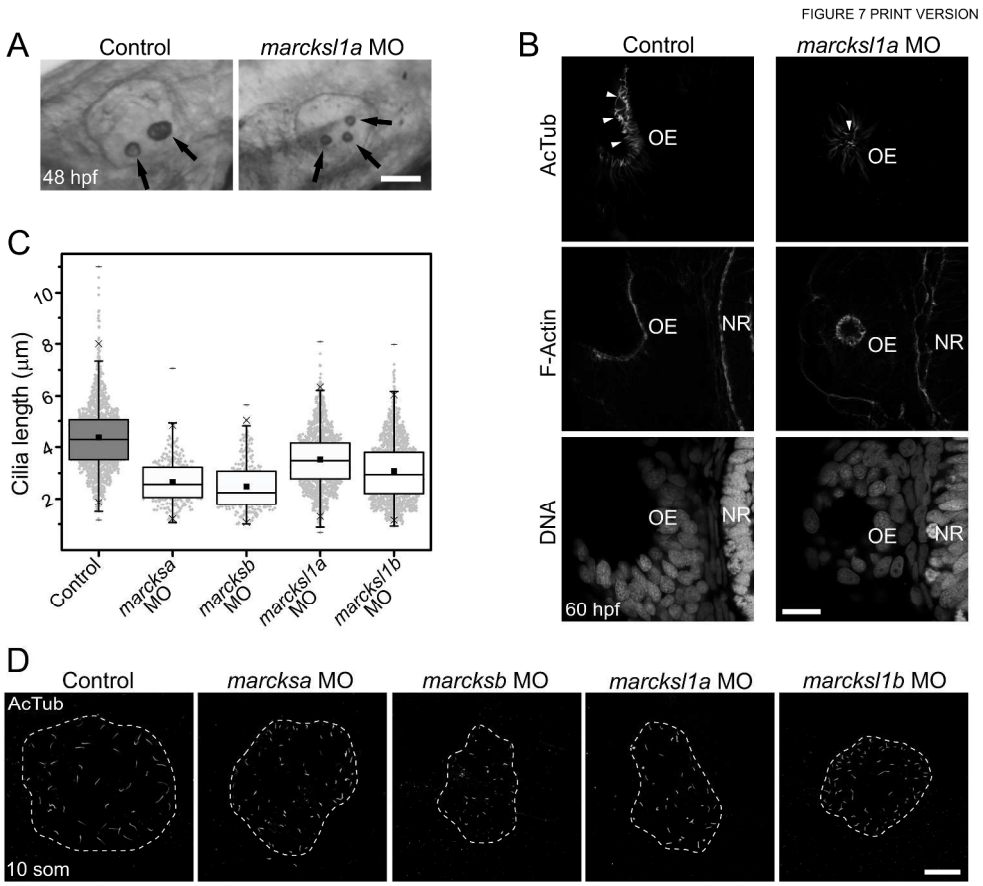

FIGURE 7. Effect of marcks genes knockdown on cilia length. (A) Bright-field images of the inner ear of control and marcksl1a-MO injected embryos at 48 hpf, showing the otoliths (arrows). (B) Confocal sections through the olfactory pit of control and marcksl1a-MO injected embryos at 60 hpf, showing cilia (arrowheads). Cilia labeled with an anti-acetylated tubulin (Ac. Tub.) antibody; F-Actin labeled with TRITC-phalloidin; DNA labeled with methyl green. OE, olfactory epithelium; NR, neural retina. (C) Box-plot showing the effect of marcks-family genes knockdown on Kupffer's vesicle cilia length. All morphant embryos have cilia significantly shorter than control at $p<0.0001$ (Student's t test). Numbers of cilia measured: control, 1575 (52 embryos); marcksa MO, 304 (11 embryos); marcksb MO, 289 (11 embryos); marcksl1a MO, 1405 (34 embryos); marcksl1b MO, 1485 (29 embryos). (D) Example confocal sections through Kupffer's vesicle (dashed line) from 10-somite embryos, showing the effect of marcks-family genes knockdown on cilia. Cilia labeled with an anti-acetylated tubulin (AcTub) antibody; and, in the online color version, centrosomes labeled with an anti-gamma tubulin (γTub) antibody. Doses of MO are like in Figure 3. Scale bars: A, 25 µm; B, 15 µm; D, 25 µm.
340x306mm (300 x 300 DPI)

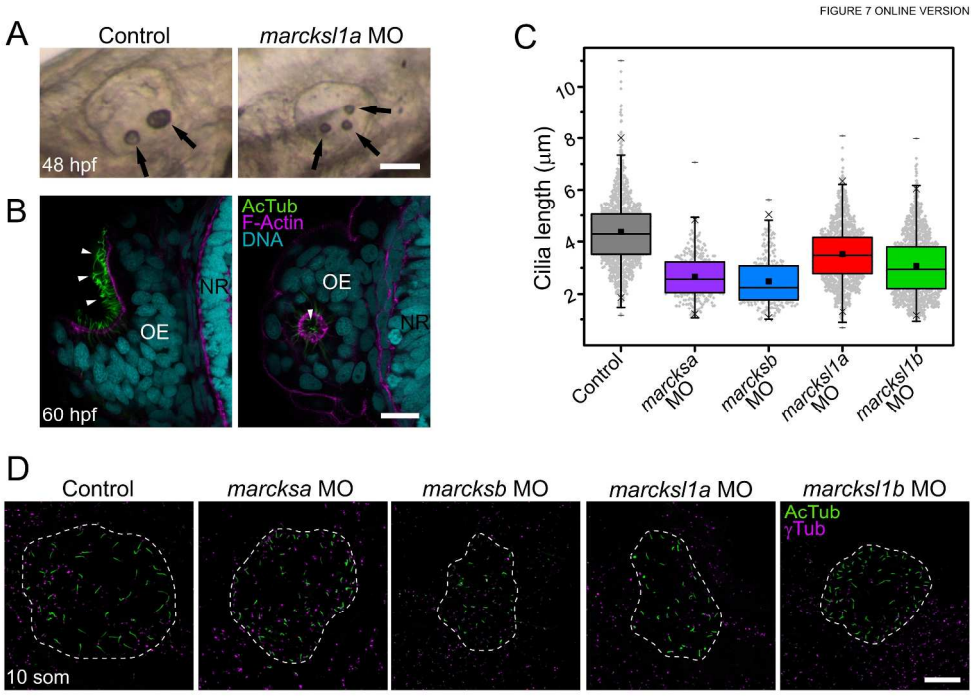

FIGURE 7. Effect of marcks genes knockdown on cilia length. (A) Bright-field images of the inner ear of control and marcksl1a-MO injected embryos at 48 hpf, showing the otoliths (arrows). (B) Confocal sections through the olfactory pit of control and marcksl1a-MO injected embryos at 60 hpf, showing cilia (arrowheads). Cilia labeled with an anti-acetylated tubulin (Ac. Tub.) antibody; F-Actin labeled with TRITC-phalloidin; DNA labeled with methyl green. OE, olfactory epithelium; NR, neural retina. (C) Box-plot showing the effect of marcks-family genes knockdown on Kupffer's vesicle cilia length. All morphant embryos have cilia significantly shorter than control at $p<0.0001$ (Student's t test). Numbers of cilia measured: control, 1575 (52 embryos); marcksa MO, 304 (11 embryos); marcksb MO, 289 (11 embryos); marcksl1a MO, 1405 (34 embryos); marcksl1b MO, 1485 (29 embryos). (D) Example confocal sections through Kupffer's vesicle (dashed line) from 10-somite embryos, showing the effect of marcks-family genes knockdown on cilia. Cilia labeled with an anti-acetylated tubulin (AcTub) antibody; and, in the online color version, centrosomes labeled with an anti-gamma tubulin (γTub) antibody. Doses of MO are like in Figure 3. Scale bars: A, 25 µm; B, 15 µm; D, 25 µm.
267x188mm (300 x 300 DPI)

Table 1. Structure of zebrafish *marcks* gene family

Gene	Chromosome mapping	Exons	Location (gene)	Location (mRNA)	Length (bp)	Introns	Location	Length (bp)	Genomic GC content (%)	Transcript GC content (%)
marcksa	20	3	6937-7218 3860-4781 434-886	1-282 283-1203 1204-1657	282 921 454	2	6936-4782	2156	41.97	51.77
marcksb	17	2	1543-1824 2644-4217	1-282 283-1857	282 1575	1	1825-2643	820	42.99	43.78
marcksl1a	19	2	3171-3432 726-2021	1-262 263-1558	262 1296	1	2022-3170	1150	42.19	39.27
marcksl1b	13	2	3261-3519 515-1921	1-259 260-1664	259 1405	1	1922-3260	1340	39.19	43.37